Dendritic information processing: placement and effect of GABAergic synapses, gap junctions, and voltage-gated ion channels on cortical neurons

Ph.D. thesis

Andrea Lőrincz

Supervisors:

Gábor Tamás, Ph.D.

Department of Comparative Physiology,
University of Szeged,
Szeged

Zoltán Nusser, D. Phil., D.Sc.

Laboratory of Cellular Neurophysiology,
Institute of Experimental Medicine,
Budapest

2003

Szeged

Table of Contents

1. General introduction

Nerve cells of the cerebral cortex possess an astonishingly complex dendritic tree, on which they receive thousands of synaptic inputs from different sources. Historically, dendrites were considered to be only surface enlarging structures with receptive function. However, theoretical studies in combination with new imaging and electrophysiological techniques developed in the last decades have revealed that elaborately branching dendrites are able to integrate thousands of synaptic inputs and permit complex spatio-temporal interactions, which may enhance the computational power of individual neurons. After a brief overview of initial steps in dendritic research, factors that determine the integrative function of dendrites will be summarized: the passive electrotonic cable properties, the dendritic morphology, the placement and dynamics of excitatory and inhibitory synaptic inputs, and the distribution of voltage-gated ion channels on the dendritic tree. The latter two factors are of central focus of my thesis. The majority of the inhibitory synapses derive from local GABAergic interneurons. Although 20 % of synapses are GABAergic in the cerebral cortex, their function is still not well understood. This could be partially explained by the large diversity of GABAergic interneurons and the difficulty of their exact classification. The functional impact of inhibitory synapses is dependent on their exact subcellular location (chapter 4 and 5), the properties of the postsynaptic receptors (chapter 4) and on the distribution of voltage gated-ion channels (chapter 6) they interact with.

Brief history of dendritic research

Information flow within the neuron

Deiters (Deiters, 1865) realised that neurons have two morphologically different processes: axons and dendrites. Camillo Golgi was the first who visualized neurons entirely with their axons and dendrites (Golgi, 1886)~~(Golgi, 1886)~~. He believed that networks of axonal collaterals carry out information processing and dendrites only provide nutrients to support neurons. Ramon y Cajal (Cajal, 1894) ~~(Cajal, 1894)~~ established the basis of modern neuroscience with his anatomical observations based on the enormous number of reconstruction of several cell types of different brain areas and mapping their afferent and efferent connectivity. He observed in the olfacory bulb that primary olfactory afferents terminate on distal dendrites of the mitral cells, therefore he concluded that the only way to activate mitral cell axons is by transmission through mitral cell dendrites (Cajal, 1894)~~(Cajal,~~

1894). He suggested the (input)-dendrite-soma-axon-synapse-(output) direction of information flow. Modern electrophysiological studies have confirmed that synaptic potentials spread through the dendrites to the cell body, axon hillock and into the axon initial segment, where impulses are generated and propagate to the axon terminals to activate synapses. Basic functions carried out by neurons are shown in figure 1.1.

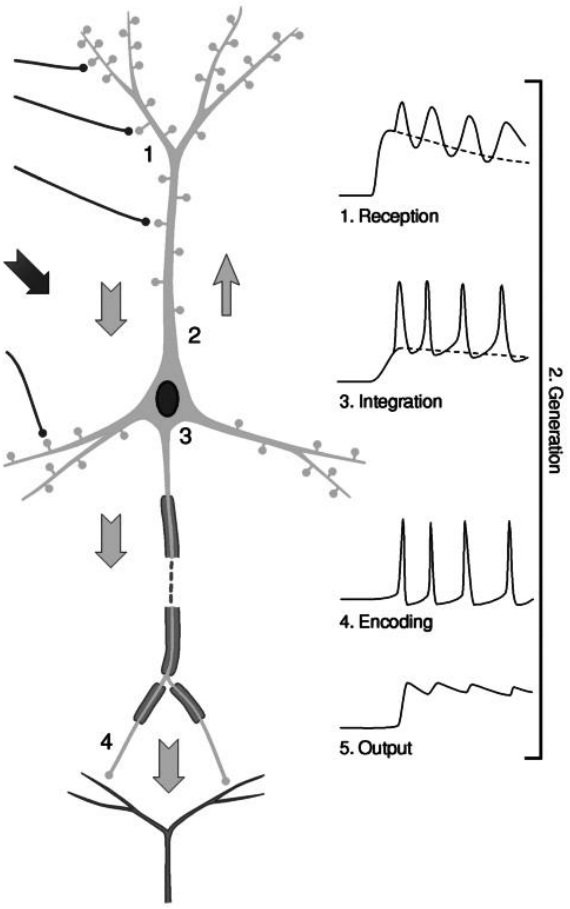

Figure 1.1. **Nerve cells have four main regions and five main functions.** 1. Reception of synaptic inputs (mostly in dendrites; to some extent in cell bodies; in some cases in axon terminals). 2. Generation of intrinsic activity at any given site on the neuron through voltage-gated membrane properties and internal second-messenger mechanisms. 3. Integration of synaptic responses with intrinsic membrane activity. 4. Generation of patterns of impulse discharges in axon, cell body, encoding outputs from cell. 5. Distribution of synaptic outputs (mostly from axon arborizations; in some cases from cell bodies and dendrites. Adapted from (Zigmond et al., 1999)(Zigmond et al., 1999).

Point neuron hypothesis

Cortical neurons communicate with each other primarily through synapses made onto their dendritic trees. Dendrites are morphologically and functionally complex, elaborate processes originating from neuronal somata. Their shape and size varies and develop parallel with the development and maturation of nerve cells. Dendrites can be highly branched structures and can be decorated with thousands of spines. Dendrites were historically considered to be only surface increasing appendages of cell bodies, providing more sites for synaptic inputs and have only a structural role in forming and segregation of synaptic inputs. In the first half of the 1990`s neuroscientists focused their attention to analyse neuronal axons. It was a common practise to consider individual neurons as simple one-compartment summing units, where all synapses have equal opportunity to influence neuronal output (Shepherd, 1990)~~(Shepherd??)~~. Somata together with dendrites were neglected or reduced to a single node, axon collaterals to wires and axon terminals to connectors. This default view is called the `point neuron` hypothesis (McCullogh and Pitts, 1943)~~(McCullogh and Pitts, 1943)~~.

Passive dendrites

In the 1950`s, by constructing the law of cable theory, Wilfred Raw introduced the concept of electrotonic structure of dendritic trees (Rall, 1958) ~~(Rall, 1958)~~ and defined the basic cable parameters: Rm: specific membrane resistance; Cm: specific membrane capacitance; Ri: axial resistance. The asymmetric cable properties along dendrites filter postsynaptic potentials. In addition, a certain percentage of synaptic current flows out via leaky dendritic membrane. As a result, the postsynaptic potentials attenuate, are delayed and their time course changes as they spread along the dendrites. Rall`s analysis predicted that synapses could be distinguished on the bases of dendritic location and that the impact of individual synapses decreases with the distance from the soma (Rall, 1977; Spruston et al., 1994)~~(Rall, 1977; Spruston et al., 1994)~~. Cable parameters were determined by patch clamp techniques (Spruston et al., 1994; Stuart and Spruston, 1998)~~([Stuart, 1998 #106], Spruston, 1994)~~, and computer models implemented cable equations in compartmental models (De Schutter, 1992)~~(De Schutter, 1992)~~.

Active dendrites

In the era of passive dendrites it was proposed that dendrites could actively amplify synaptic inputs (Lorente de Nó and Coundouris, 1959)~~(Lorente de Nó and Coundouris, 1959)~~. Several

experimental observations provided evidence that dendrites can generate active events. Eccles et al. found spike like responses in motorneurons (Eccles et al., 1958)~~(Eccles et al., 1958)~~, intracellular recording from dendrites of Purkinje cells

demonstrated the existence of dendritic spikes (Llinás et al., 1968; Llinás and Nicholson, 1971), and Spencer and Kandel ~~(Llinás et al., 1968; Llinás and Nicholson, 1971) and Spencer and Kandel (1961)~~ described regenerative fast prepotentials with assumed distal dendritic origin in hippocampal pyramidal cells (Spencer and Kandel, 1961)~~(Spencer and Kandel, 1961)~~. Active properties of dendrites are determined by voltage-gated ion channels. Intracellular recording of dendritic Ca^{2+}- spikes and somatic Na^{+}-spikes (Llinás and Sugimori, 1980)~~(Llinás and Sugimori, 1980)~~ suggested the existence of voltage-gated ion channels on the somatodendritic surface. These early and elegant experiments suggested a rich repertoire of dendritic active conductances.

Integrative function of dendrites is determined by several factors

Multiple forms of dendritic excitability

The final output of the neuron, the action potential (AP) is initiated, under most circumstances, in the axon, because the threshold for generating action potential is the lowest in the axon itself (Stuart and Sakmann, 1994; but see dendritic sodium and calcium spikes, Hausser, 2000)~~(Stuart and Sakmann, 1994)Hausser et al., 2000~~. However, somatic action potentials can backpropagate to dendrites in certain neurons (Stuart and Hausser, 1994; Stuart and Sakmann, 1994)~~(Stuart and Hausser, 1994; Stuart and Sakmann, 1994)~~. Furthermore, the axonal sodium AP initiation zone can be shifted to proximal dendrites (Turner et al., 1991)~~(Turner et al., 1991)~~ and distal dendritic Na^{+} and Ca^{2+} spikes can be initiated by increased, simultaneous synaptic stimulation (reviewed by Stuart et al., 1997; Hausser et al., 2000)~~(Stuart et al., 1997; Hausser et al., 2000)~~ resulting more than one spike initiation zone. Backpropagating APs inform dendrites about the axonal output and facilitate dendritic neurotransmitter release (Hausser et al., 2000)~~(Hausser et al., 2000)~~, dendritic Ca^{2+} spikes serve as coincidence detectors of synaptic inputs and neuronal outputs. Dendritic Ca^{2+} spikes can occur without triggering an axonal action potential, and axonal APs don't propagate fully into dendrites in many neurons (Vetter et al., 2001)~~(Vetter et al., 2001)~~. These events are incompatible with the point neuron hypothesis and contributed to the development of the two-compartment view of neuron. That is, a cell consists of a proximal compartment, where axonal APs are generated, and a distal dendritic compartment, where

calcium spikes are generated. Experiments investigating the relationship between the electrical compartments revealed that these compartments are not static, but rather dynamic and interact with each other. For example, backpropagating action potentials can lower the threshold for initiation of distal calcium spikes, thus enabling layer 5 pyramidal cells to couple different synaptic inputs, if they arrive in a narrow time window (backpropagation activated firing: BAC firing). In layer 5 pyramidal cell a third compartment was introduced, that modulate the interaction between somatic and dendritic spike initiation zones (Larkum et al., 1999, 2001)~~(Larkum et al., 1999, 2001)~~.

Propagation of the active processes, including backpropagating APs and dendritic spikes and the interaction between them vary in different cell types. This is mainly the consequence of the diversity in dendritic morphology and distribution of voltage-gated ion channels in different types of neurons.

Dendritic morphology

Since the studies of Cajal, morphology has been one of the main criteria for defining neuronal cell classes. The large morphological variability in dendritic trees raises the question on its functional role. In the age of the point neuron hypothesis, when only receptive function was attributed to dendrites, it was thought that wiring of dendritic trees was constructed to occupy minimal space according to the space limitation of brain. In addition, long, branching dendrites increase the cell's ability to get inputs from different layers (Koch and Segev, 2000)~~(Koch and Segev, 2000)~~. However, morphological diversity is paired with different types and expression of ion channels making hard to investigate its pure functional significance. Applying the same pattern of voltage-gated ion channels in a modelling study, as a function of morphology Vetter et al. have found (Vetter et al., 2001)~~(Vetter et al., 2001)~~ differences in the propagation of active dendritic processes between different cell types. Even within the same cell class different branching pattern and geometry of oblique dendrites can contribute specifically to functional diversities (Schaefer et al., 2003)~~(Schaefer et al., 2003)~~.

The smallest structures emerging from dendrites are spines. Most of them consist of a short or long spine neck, at the end of which the spine head locates. Dendritic spines are the major targets of excitatory glutamergic synapses of pyramidal cells in the cerebral cortex (Peters et al., 1991)~~(Peters et al., 1991)~~, therefore revealing their functional roles is essential for understanding synaptic integration and dendritic information processing. Spines show a large

diversity in size and shape. Majority of the spines have small, stubby, mushroom or branched, multiple lobe structure in the brain (Peters et al., 1991; Harris, 1999)~~(Peters et al., 1991; Harris, 1999)~~. The functional significance of various shapes is still not well understood. From an electrical point of view, the smaller size and narrower spine neck results in higher input resistance and smaller capacitance giving a larger amplitude and faster kinetics to the synaptic response evoked on spines (Shepherd, 1990; Shepherd, 1996)~~(Shepherd, 1990; Shepherd, 1996)~~. Thus, depending on the geometry of mainly spine necks, spines are more or less electrically isolated from dendritic shafts. An important intracellular organelle of dendritic spines, the smooth endoplasmic reticulum forms spine apparatus (SR) and serves as local store for Ca^{2+} ions and secondary messenger molecules. Polyribosomes in spines ensure local protein synthesis during developmental synaptogenesis (Steward et al., 1996)~~(Steward et al., 1996)~~ and synaptic plasticity (Yamazaki et al., 2001)~~.Yamazaki et al., 2001).~~ These factors together with several other processes (Shepherd, 1996)~~(Shepherd, 1996)~~ make spines the smallest electrically and biochemically isolated compartments in dendritic tree (Shepherd, 1990; Shepherd, 1996) the basic units of synaptic integration (Yuste and Denk, 1995)~~(Yuste and Denk, 1995)~~.

Distribution of dendritic voltage-gated ion channels

The integrative function of neurons highly depends on the properties and somato-dendritic distribution of voltage-gated ion channels. Dendrites of nerve cells express numerous types of voltage-gated ion channels and both functional and pharmacological properties of these channels are extensively studied by cellular neurophysiology. Sodium and potassium channels in dendrites are responsible for the active propagation of APs from the axon into the dendrites (back-propagation). The molecular structure and dendritic location of these channels control the shape and amplitude of backpropagating APs, the amplitude of EPSPs and overall dendritic excitability (Johnston et al., 2000)~~(Johnston et al., 2000)~~. Calcium channels are responsible for local changes in dendritic calcium concentrations following back-propagating APs and synaptic potentials. Direct somatic and dendritic patch-clamp (Stuart and Sakmann, 1994) ~~(Stuart and Sakmann, 1994)~~ measurements directly revealed several types of voltage-gated currents in dendrites (Migliore and Shepherd, 2002)~~(Migliore and Shepherd, 2002)~~. Uniform distributions of Na^+- (Magee and Johnston, 1995)~~(Magee and Johnston, 1995)~~, K^+- (Bischofberger and Jonas, 1997)~~(Bischofberger and Jonas, 1997)~~ and Ca^{2+}-currents (Bischofberger and Schild, 1995)~~(Bischofberger and Jonas, 1997)~~ as well as non-uniform distribution of Na^+- (Stuart and

Hausser, 1994)(Stuart and Hausser, 1994), A- (Johnston et al., 2000)(Johnston et al., 2000), H-currents (Maccaferri and McBain, 1996; Magee, 1998), (Maccaferri and McBain, 1996; Magee, 1998), and L-, and N-type Ca^{2+}-currents (Bischofberger and Schild, 1995)(Bischofberger and Schild, 1995) were reported. Voltage-gated ion channels can be distributed in cell type specific manner, thus integrative properties and firing behavior vary from cell type to cell type (Magee, 1999b)(Magee, 1999b). For example, Na^{+}- channels are more or less excluded from Purkinje cell dendrites, whereas have a high density in pyramidal cell dendrites. The distribution of these channels determines how axo-somatically initiated sodium APs propagate actively into the dendrites (Stuart and Sakmann, 1994; Magee, 1999b)(Stuart and Hausser, 1994; Magee, 1999b).

A number of regulatory systems can differently modulate dendritic ion channels along the somatodendritic surface. For example, activation of protein kinases leads to a fast recovery from slow inactivation of Na+-channels (Colbert and Johnston, 1998; Tsubokawa, 2000)(Colbert and Johnston, 1998; Tsubokawa, 2000) and downregulation of transient K+-channels result in an increased excitability (Hoffman and Johnston, 1998) (Hoffman and Johnston, 1998) in the distal dendrites. Therefore, a non-uniform distribution of a current along the somato-dendritic axis may represent an uneven channel density or regulation.

As for the anatomical approaches, most of our knowledge on the distribution of voltage-gated ion channels come from light microscopic immunfluorescence (McNamara et al., 1993; Sekirnjak et al., 1997)(McNamara et al., 1993; Sekirnjak et al., 1997) and immunoperoxidase (Rhodes et al., 1996)(Rhodes et al., 1996) studies. However, these methods have high sensitivity, sometimes it's hard to determine whether cytoplasmic or plasma membrane-attached ion channels are labelled. Electronmicroscopical immunoperoxidase studies of K+-channel subunits Kv4.2 (Alonso and Widmer, 1997)(Alonso and Widmer, 1997) and Kv3.1 (Sekirnjak et al., 1997)(Sekirnjak et al., 1997) revealed first plasma membrane attached immunoreactivity. However because of the diffusible nature of the reaction end-product of the peroxidase enzyme reaction, this method is not suitable for quantitative comparision of antigens in different compartments. Using non-diffusible gold particles coupled to the secondary antibody, preembedding and postembedding immunogold methods are more suitable for high-resolution localisation of molecules (Nusser, 1999)(Nusser, 1999). In chapter 6 we applied preembedding-immunogold method to analyse quantitatively the subcellular distribution of HCN1, a subunit of hyperpolarization activated and cyclic nucleotid dependent ion channel (Ludwig et al., 1998;

Magee, 1998; Santoro et al., 1998; Moosmang et al., 1999)~~(Ludwig et al., 1998; Magee, 1998; Santoro et al., 1998; Moosmang et al., 1999)~~. The limitations of this method will be discussed.

Placement of synaptic inputs

As described previously, passive electrotonic properties, complexity of dendritic morphology together with the distribution of active conductances are the key determinants of the integrative functions of dendrites. Because of their dynamic nature, these factors make dendrites highly compartmentalised (Hausser and Mel, 2003)~~(Hausser and Mel, 2003)~~ structures able to perform dynamic changes according to the actual network activity. Synaptic inputs arriving to distinct parts of the dendritic tree therefore can have different effects on the neuronal output and/or the dendritic excitability depending on their location (Williams and Stuart, 2002, 2003a, b) ~~(Williams and Stuart, 2003a, b)~~.

Owing to the filtering properties of electrotonic structure and morphology of dendritic tree, synaptic inputs arriving to distal dendrites attenuate in amplitude (Rall, 1977)~~(Rall, 1977)~~. However, there are mechanisms equalizing this filtering effect (Williams and Stuart, 2003a)~~(Williams and Stuart, 2003a)~~. For example, boosting the effectiveness of distal synapses can be achieved by increasing the number of postsynaptic receptors (Spruston et al., 1995; Andrasfalvy and Magee, 2001)~~(Spruston et al., 1995a; Andrasfalvy and Magee, 2001)~~, or by NMDA receptor mediated Ca2+ spikes (Oakley et al., 2001; Oviedo and Reyes, 2002)~~(Oakley et al., 2001; Oviedo and Reyes, 2002)~~. Dendritic hyperpolarization activated current I_h (Williams and Stuart, 2000; Berger et al., 2001)~~(Williams and Stuart, 2000; Berger et al., 2001)~~ normalizes the time course of EPSPs, making it independent of the location of synapses. In spite of the presence of these counterbalancing events, functional impact of distal EPSPs shows cell type specific differences *in vitro* (Magee and Cook, 2000; Williams and Stuart, 2002)~~(Magee and Cook, 2000; Williams and Stuart, 2002)~~, and *in vivo* it also depends on the ongoing synaptic activity (Bernander et al., 1991; Pare et al., 1998)~~(Bernander et al., 1991; Pare et al., 1998)~~. Only the functional effects of distal excitatory inputs have been investigated extensively (Williams and Stuart, 2003a)~~(Williams and Stuart, 2003a)~~, however 20 % of synaptic inputs arrive from inhibitory GABAergic interneurons. The impact of dendritic inhibitory inputs is poorly understood (Williams and Stuart, 2003b)~~(Williams and Stuart, 2003b)~~.

Dendritic inhibition is mediated by GABAergic cells

Sources of synaptic inputs

Dendrites receive thousands of excitatory and inhibitory inputs from subcortical areas and from the two main cell types of the neocortex. Pyramidal cells are the major cortical output cells constituting about 80% of neurons in the neocortex. They can be found in all cortical layers except layer I. Their characteristic features are spiny dendrites, a thick, radially oriented apical dendrite, forming a terminal tuft in the most superficial cortical layer and a set of basal dendrites. In addition to the projection to subcortical or other cortical areas, each pyramidal cell has an axon collateral network that forms part of the local circuitry. Using glutamate as neurotransmitter, they are responsible for the majority of EPSPs. Pyramidal cells innervate dendritic spines of pyramidal cells and dendritic shafts of aspiny interneurons.

Interneurons form 20% of cortical synapses and take place in inhibitory processes. They are heterogeneous in many aspects, but have a common feature compared to pyramidal cells, that their axons remain in the cortex, making short-range projections to pyramidal cells and other interneurons. These cells release γ-aminobutiric acid (GABA) as neurotransmitter, therefore are commonly referred as GABAergic cells.

GABAergic transmission

Majority of the interneurons in the neocortex were shown to use GABA as neurotransmitter (Somogyi and Hodgson, 1985)~~(Somogyi and Hodgson, 1985)~~. GABA released to synaptic cleft can act on two types ($GABA_A$ and $GABA_B$) of pre- and postsynaptic GABA receptors. A third type, $GABA_C$ receptor, is closely related to $GABA_A$ receptors and is expressed in the retina and visual cortex (Cutting et al., 1991)~~(Cutting et al., 1991)~~.

$GABA_A$ receptors are the members of the ligand-gated ion channel superfamily. Five subunits are assembled into a receptor with a central pore, permeable to Cl^- and to a less extent HCO_3^-. The conformational changes caused by the binding of GABA open the channel and the influx of chloride ions according to their electrochemical gradient result in either de- or hyper-polarization of the postsynaptic membrane. By lowering the memrane resistance they can shunt the more distant excitatory snaptic inputs. Activation of $GABA_A$ receptor can result in depolarizing responses in neonatal neurons and spinal cord neurons (Obata et al., 1978)~~(Obata et al., 1978)~~, however under certain circumstances in mature cortical neurons as well (Andersen et al., 1980; Cohen et al., 2002; Gulledge and Stuart, 2003)~~(Andersen et al., 1980; Cohen et al., 2002; Gulledge and Stuart, 2003)~~. $GABA_A$ receptors are formed from pentameric assemblies of eighteen subunits (α_{1-6}, β_{1-4}, γ_{1-4}, δ, ε, θ, π). Differential assembly of subunits into distinct complexes provides the basis of $GABA_A$ receptor heterogeneity.

$GABA_B$ receptors belong to the family G-protein coupled receptors and have the highest homology to metabotropic glutamate receptors. Presynaptic $GABA_B$ receptors can inhibit transmitter release via inactivation of Ca^{2+}-channels, postsynaptic receptors can inhibit the production of cAMP and by the activation of K^+-channels (Kir.3.1/3.2) evoke slow kinetic IPSPs. $GABA_B$ receptors are unique in that a functional $GABA_B$ receptor is formed by dimerization of two homologous subunits (GBR1 and GBR2). GBR1 carries the ligand-binding site and GBR2 couples to the G-protein. Multiple splice variants of GBR1 and GBR2 have been identified, suggesting structural heterogeneity.

Functional impact of different GABAergic synapses depends on the structure and type of postsynaptic GABA receptors. Presynaptic cell type specific variability in subunit composition of postsynaptic $GABA_A$ receptors has been shown (Nusser et al., 1996; Nyiri et al., 2001; Klausberger et al., 2002)~~(Nusser et al., 1996; Nyiri et al., 2001; Klausberger et al., 2002)~~. Although postsynaptic $GABA_A$ and $GABA_B$ receptor mediated responses can be evoked in the cerebral cortex by extracellular stimulation or glutamate application (Benardo, 1994)~~(Benardo, 1994)~~, GABAergic interneurons tested so far have been shown to act on postsynaptic $GABA_A$ receptors. The sources of postsynaptic $GABA_B$ receptor mediated responses are still unknown. This issue will be addressed in chapter 4.

Diversity of GABAergic interneurons

Because of their immense heterogeneity, so far it has been impossible to classify interneurons into clear, nonoverlapping populations based on their anatomical and physiological properties. Using Golgi impregnation, Ramón y Cajal (Cajal, 1904)~~(Cajal, 1911)~~ revealed the anatomical diversity of interneurons on the basis of the morphological differences in their smooth or sparsely spiny dendritic and axonal arbour. For example, large basket cells have multipolar dendrites and long vertically oriented axonal arbour, while double bouquet cells can display bipolar or bitufted dendritic morphology and their radial axons span all layers (Cajal, 1904; Peters and Sethares, 1997; Tamas et al., 1998)~~(Cajal, 1911; Peters and Sethares, 1997; Tamas et al., 1998)~~ A useful characterization of interneuron subtypes is based on their neurochemical content. Interneurons synthesize different Ca^{2+} -binding proteins (parvalbumin (PV), calretinin (CR), calbindin (CB)) and neuropeptides (somatostatin (SOM), cholecystokinine (CCK), neuropeptide-Y (NPY), and vasoactive intestinal polypeptide (VIP)). Different sets of basket cells contain PV or CCK, double bouquet cells are considered to have VIP, neurogliaform cells NPY and bitufted cells SOM (Freund and Buzsaki, 1996)~~[Freund, 1996 #7]~~. Functional characterisation is based on action potential firing patterns (Kawaguchi and Kubota, 1996, 1997; Gupta et al.,

2000)(Kawaguchi and Kubota, 1996, 1997; Gupta et al., 2000) and the facilitating or depressing nature of postsynaptic potentials evoked by short trains of presynaptic action potentials (Reyes et al., 1998; Gupta et al., 2000)(Reyes et al., 1998; Gupta et al., 2000).

Distinct classes of GABAergic interneurons innervate specific subcellular regions of postsynaptic cells, subdividing the surface of the postsynaptic cells according their target preference (Tamas et al., 1997; Somogyi et al., 1998a; Tamas et al., 1998)(Tamas et al., 1997; Somogyi et al., 1998a; Tamas et al., 1998). This property makes GABAergic cells ideal substrates for the investigation of location specific effects of inhibitory inputs. CCK or PV containing basket cells innervate perisomatic regions, PV-containing chandelier (Szentagotai) or axo-axonic cells (Somogyi et al., 1983)(Somogyi et al., 1983) target only the axon initial segment of pyramidal cells (Somogyi, 1977; Somogyi et al., 1982)(Somogyi, 1977; Somogyi et al., 1982) and other interneurons (Gulyas et al., 1999)(Gulyas et al., 1999). Having a strategically important position on the central integration unit of postsynaptic cells, near the site of action potential initiation, perisomatic inhibitory synapses can regulate the local generation of sodium action potentials (Hestrin and Armstrong, 1996; Galarreta and Hestrin, 1999; Tamas et al., 2000)(Galarreta and Hestrin, 1999; Gibson et al., 1999; Tamas et al., 2000). Dendrites receive several distinct GABAergic inputs. For example, double bouquet cells innervate distal dendritic shafts and more frequently dendritic spines (Tamas et al., 1997)(Tamas et al., 1997), but dendrite targeting cells (Tamas et al., 1997)(Tamas et al., 1997) primilarly target dendritic shafts in visual cortex. There are also cells with well characterised firing patterns, like regular spiking nonpyramidal (RSNP) cells and late-spiking (LS) cells (Cauli et al., 1997; Kawaguchi and Kubota, 1997; Cauli et al., 2000; Gupta et al., 2000)(Cauli et al., 1997 Gupta, 2000 #50; Kawaguchi and Kubota, 1997; Cauli et al., 2000), probably innervating dendritic regions, but their subcellular target selectivity is unknown. Dendritic inhibitory synapses can interact with voltage-gated ion channels (Williams and Stuart, 2003b)(Williams and Stuart, 2003b), shunt excitatory synapses distal to the soma (Hoffman and Johnston, 1998)(Hoffman and Johnston, 1998), shunt backpropagation of Na^+-dependent action potential (Spruston et al., 1995)(Spruston et al., 1995b), control synaptic plasticity, and regulate dendritic Ca^{2+} spikes (Miles et al., 1996)(Miles et al., 1996). In spite of the abundance of GABAergic cells innervating dendritic regions comparing to the perisomatic ones, their distinct, cell type specific impact on the excitability and/or output of postsynaptic cells is not well understood. We investigated this

question in chapter 4 and 5 with special regard to the exact location of synapses on the somatodendritic surface.

Intercellular communication between interneurons

Chemical synapses are the most common form of communication in the mammalian central nervous system. Excitatory axon terminals establish Type I. (Gray) or asymmetric synapses on dendritic spines and shafts, with the characteristic feature of large postsynaptic density. GABAergic interneurons make Type II. (Gray) or symmetric synapses primarily on dendritic shafts and somata according to their target specificity.

Another type of communication is transferred via electrical synapses, where chemical transmitter is not released. Its structural correlate, the gap junction, is composed from parallel patches of closely apposed membranes, providing a narrow, 8-9 nm wide cleft (Sloper and Powell, 1978; Peters et al., 1991)~~(Sloper and Powell, 1978; Peters et al., 1991)~~. Connexins, the building proteins of gap junctions are highly expressed in the developing brain (Connors et al., 1983)~~(Connors et al., 1983)~~. Although decline in number, they are still present in the adult brain and the question of their specific role has challenged scientists. Activation of an interneuron results in inhibitory responses in postsynaptic interneurons if they chemically coupled, but excitatory spikelets are triggered if they are electrically coupled (Hestrin and Armstrong, 1996; Galarreta and Hestrin, 1999)~~(Galarreta and Hestrin, 1999; Gibson et al., 1999)~~. Gap junctions allow current to pass directly between adjacent cells, and since synaptic release and receptor mechanisms are not involved, the synaptic delay is shorter than that of chemical transmission. Gap junctions were theoretically (Traub et al., 2001)~~(Traub et al., 2001)~~ and experimentally (Hestrin and Armstrong, 1996; Draguhn et al., 1998; Galarreta and Hestrin, 1999)~~(Draguhn et al., 1998; Galarreta and Hestrin, 1999; Gibson et al., 1999)~~ proved to contribute to synchronous activity of interneuron networks. Although the presence of gap junctions (Sloper and Powell, 1978)~~(Sloper and Powell, 1978)~~ and different types of connexins (Condorelli et al., 2000; Rozental et al., 2000; Rouach et al., 2002) ~~(Condorelli et al., 2000; Rozental et al., 2000; Rouach et al., 2002)~~ were shown in the cerebral cortex, direct anatomical evidence for electrical coupling between interneurons has been provided only between parvalbumin immunreactive basket cells in hippocampus (Fukuda and Kosaka, 2000)~~(Fukuda and Kosaka, 2000)~~ and neocortex (Tamas et al., 2000; Fukuda and Kosaka, 2003)~~(Tamas et al., 2000; Fukuda and Kosaka, 2003)~~. Together

with its role in synchronous activity, direct anatomical evidence will be provided for dendro-dendritic gap junctions in the network of interneurons targeting dendrites in chapter 5.

2. Aims and contributions

Two factors determining dendritic information processing were studied in this thesis: **placement of inhibitory synapses** and **distribution of voltage-gated ion channels**.

Our specific aims were:

1. to classify GABAergic interneurons terminating on dendrites (Chapter 4, 5).

2. to reveal the number and subcellular position of the synapses of dendrite targeting cells on identified postsynaptic cells (Chapter 4, 5)

3. to investigate whether the effect of different dendrite targeting interneurons is related to the subcellular position of their synapses on the postsynaptic cell (Chapter 4, 5)

4. to determine the subcellular distribution of HCN1 in cortical pyramidal cells (Chapter 6)

Contributions:

In chapters 4 and 5, whole-cell patch-clamp recordings were performed by János Szabadics and Gábor Tamás. I performed the anatomical characterisation of interneurons, light- and electron-microscopic (EM) mapping of dendritic gap junctions and GABAergic synapses in Chapters 4 and 5. I also carried out all immunohistochemical experiments in Chapter 6.

3. Materials and methods

Electrophysiology

Slices were obtained from Wistar rats (P19-35) and maintained as described (Tamas et al., 2000)~~(Tamas et al., 2000)~~. Whole-cell patch clamp recordings were carried out at ~35 °C from concomitantly recorded pairs, triplets or quadruplets of layers 2-3 putative interneurons and/or pyramidal cells as detailed previously. Micropipettes (5-7 MΩ) were filled with (in mM) 126 K-gluconate, 4 KCl, 4 ATP-Mg, 0.3 GTP-Na2, 10 HEPES, 10 creatine phosphate and 8 biocytin (pH 725; 300 mOsm). Signals were recorded with HEKA EPC9/2 amplifiers in fast current clamp or whole cell mode and were filtered at 5 kHz, digitized at 10 kHz and analyzed with PULSE software (HEKA, Lambrech/Pfalz, Germany). Presynaptic cells were stimulated with brief (2 ms) suprathreshold pulses. During control conditions and pharmacology, postsynaptic cells were held at -50 ± 4 mV membrane potential; traces shown are means ± s.e. (gray) of averages derived from 20-50 episodes of individual paired recordings. Mann-Whitney U-test was used to compare datasets, differences were accepted as significant if $p < 0.05$.

Phasing paradigm

Presynaptic RSNP cells were stimulated with brief (2 ms) suprathreshold pulses at 60 ms intervals (16.6 Hz) for the paired pulse protocol and at 19 and 37 Hz for the beta and gamma frequency phasing paradigm. Depression/facilitation of EPSPs or IPSPs fully develops only after 4 or more postsynaptic events, therefore we used 6-10 presynaptic cycles in order to test the effect of the use-dependent modification of PSPs on the phasing of postsynaptic activity. We applied the same paradigm throughout the study for consistency. Trains were delivered at >5s intervals, to minimize intertrial variability. During subthreshold paradigms, postsynaptic cells were held at –51 ± 4 mV membrane potential. For phasing trials, they were depolarized with constant current injections just above threshold so as to elicit firing. Unless specified, traces shown are averages of 30-200 episodes. The amplitude of postsynaptic events was defined as the difference between the peak amplitude and the baseline value measured prior to the PSP onset. Firing probability plots were constructed from 50-100 consecutive trials as follows: within the interval separating two presynaptic action potentials, postsynaptic spike latencies were measured

from the peak of the preceding presynaptic action potential. Subsequently, the data were pooled from cycles according to the characteristics of the postsynaptic responses (see Results in chapter 5). Controls were collected prior to the onset of the presynaptic spike train using identical cycle duration and data obtained during presynaptic activation were normalized to control. Data are given as mean ± s. d. Mann-Whitney U-test and Friedman-test was used to compare datasets, differences were accepted as significant if $p \leq 0.05$. Connections were classified by cluster analysis based on postsynaptic cell firing probability (Statistica for Windows, StatSoft, USA). Joining trees were constructed by Ward's method of amalgamation and were based on Euclidean distances.

Histological processing of biocytin filled cells

Histology and anatomical evaluation were performed as described in Tamas et al., 1997 (Tamas et al., 1997)~~(Tamas et al., 1997)~~. Depolarizing current pulses employed during recording resulted in an adequate filling of neurones by biocytin. Slices were sandwiched between two Millipore filters to avoid deformations and fixed in 4% paraformaldehyde, 1.25 % glutaraldehyde and 15 % picric acid in 0.1 M phosphate buffer (PB) (pH 7.4) for at least 12 hours. After several washes in 0.1 M PB, slices were cryopected in 10%, then 20 % succrose in 0.1 M PB. Slices were freeze-thawed in liquid nitrogen, then embedded in 10 % gelatine. 300 µm thick slices embedded in gelatine blocks were resectioned at 60 µm thickness. Sections were incubated in avidin-biotin-horsradish peroxidase (ABC; Vector Labs) complex made in TBS (1:100, pH 7.4) at 4° C overnight. The enzyme reaction was revealed by 3'3-diaminobenzidine tetrahydrochloride (0.05 %) as chromogen and 0.01% H_2O_2 as oxidant. Sections were postfixed with 1 % OsO_4 in 0.1 M PB. After several washes in distilled water, sections were stained in 1 % uranyl acetate, dehydrated in ascending series of ethanol. Sections were infiltrated with epoxy resin (Durcupan, Fluka) overnight and embedded on glass slices (Tamas et al., 1997).~~(Tamas et al., 1997)~~

Anatomical evaluation of recovered cells

Three-dimensional light microscopic reconstructions of recovered cells were carried out using Neurolucida (MicroBrightfield, Colchester, VT) with 100x objective from the 60 µm thick serial sections. Dendrogram constructions and synaptic distance measurements were aided by Neuroexplorer (MicroBrightfield) software. The entire somatodendritic surface of recorded cells were tested for close appositions with filled axons or filled dendrites, each of which was traced

back to the parent soma. Because the resolution of light microscope (200 nm) is not sufficient for the precise identification of synaptic connection, all of the found close appositions were tested in electron microscope. Light micrographs taken from each close apposition in different focal depth were used for the exact identification of these presumed synaptic connections under electron microscope. Blocks containing the cells were cut out from the sections on slides and reembedded. 70 nm serial sections were cut with an ultramicrotome (Leica Ultracut R; Leica Mirosystems, Vienna, Austria and RMC MTXL; Boeckeler Instruments, Tucson, Arizona) and mounted on Pyloform-coated copper grids and stained with lead citrate (EM Stain; Leica Mirosystems). Light microscopically detected presumed synapses were checked on the ultrathin sections in electron microscope. We used the following criteria for the identification of synaptic junctions: 1, accumulation of synaptic vesicles in the presynaptic terminal; 2, rigid membrane apposition between the pre- and postsynaptic membranes, with the characteristic widening of extracellular space (synaptic cleft); 3, postsynaptic specialization. Direct membrane appositions alone didn't predict the presence of synaptic junction.

Random sampling of postsynaptic targets

Axon rich areas, including all layers covered by the axonal field, were cut out from sections on the slide and re-embedded for ultrathin sectioning. 70 nm serial sections were scanned under electron microscope and biocytin filled axon profiles were followed until they established synaptic connections with unlabelled postsynaptic profiles. Since all profiles were followed and the plane of the section randomly cuts through axonal branches, the above procedure ensured a random sample of postsynaptic targets. Tracing of serial sections were also used for the identification of postsynaptic target. Dendritic spines contain smooth endoplasmic reticulum or as called spine apparatus, but lack in the most cases mitocondria (Tamas et al., 1997)~~(Tamas et al., 1997)~~. Postsynaptic profiles containing mitochondria and/or microtubules were identified as dendritic shafts.

Immunohistochemistry of HCN1

Preparation of the antibodies

Our collaborators developed a guinea pig polyclonal antibody (N12) against a glutathion S-transferase fusion protein containing the C-terminus of rat HCN1 (amino acid residues 850-910) using a method described earlier (Shigemoto et al., 1997)~~(Shigemoto et al., 1997)~~. The fusion

protein was purified by preparative sodium dodecyl sulphate–polyacrylamide gel electrophoresis (SDS-PAGE) for immunization. Excised gels containing the purified fusion protein were emulsified with Freund's complete adjuvant (Nacalai tesque, Kyoto, Japan) and injected subcutaneously into guinea pigs (50-100μg fusion protein per animal). After 4 weeks, the fusion protein was injected again with Freund's incomplete adjuvant. From antisera collected 2 weeks after the second injection, HCN1 antibody was affinity-purified using a CNBr-activated glutathion Sepharose 4B (Amersham Pharmacia Biotech, Upsala, Sweden) coupled to the purified fusion protein. The rabbit polyclonal antibody to HCN1 was purchased from Alomone Labs. (Jerusalem, Israel) and was raised against the N-terminus of the rat HCN1 (amino acid residues 6-24).

Immunoblotting

Crude membrane fractions of the whole brain were prepared from adult male rats (Sprague-Dawley, Charles River, Japan) as described previously (Shigemoto et al., 1997). The membrane fractions were separated by 7.5% SDS-PAGE and transferred to nitrocellulose membranes (Bio-Rad, Hercules, CA, USA). The membranes were blocked with Block-Ace (Dainippon Pharmaceutical, Suita, Japan) and then reacted with the rabbit (0.5 μg/ml) and guinea pig (0.2 μg/ml) HCN1 antibodies. An alkaline phosphatase-labeled secondary antibody (Chemicon, Temeculla, CA, USA) was used to visualize the reactions.

The immunoreactivity completely disappeared after preincubation of these antibodies with the respective antigens, indicating that both antibodies specifically react with rat HCN1 (**Fig. 1**).

Preparation of tissue for immunocytochemistry

Sixteen adult (P35-67) male Wistar rats were deeply anaesthetized with ketamine (30 mg/kg) and xylazine (10 mg/kg). Thirteen rats were perfused through the aorta with 0.9% saline for 1 min., followed by ice-cold fixatives, containing either 4 % paraformaldehyde, 0.05 % glutaraldehyde, and 15 v/v% picric acid; or 4 % paraformaldehyde and 15 v/v% picric acid made up in 0.1 M phosphate buffer (PB, pH=7.4) for 11-30 min. The brains were immediately removed and blocks were cut out from the forebrain and were kept in 0.1 M PB. Three animals were perfused first with 0.9% saline for one min., followed by a fixative containing 4% paraformaldehyde and 1% glutaraldehyde in 0.1 M sodium acetate buffer (pH=6.0) for 2 minutes, followed by an hour fixation with a fixative containing 4% paraformaldehyde and 1% glutaraldehyde in 0.1 M sodium borate buffer (pH=8.0, Sloviter et al., 2001). After the perfusion, the brains were left in the skull

for 24 hours at 4 °C. The brains were then removed and horizontal sections (60 µm in thickness) were prepared with a Vibratome (VT1000S, Leica Microsystems, Vienna, Austria), were collected and washed several times in 0.1 M PB.

Pre-embedding immunocytochemistry

Normal goat serum (NGS, 10%) in Tris-buffered saline (TBS, pH=7.4) was used for blocking, followed by incubations in the primary and secondary antibodies as described earlier (Nusser et al., 1995)~~(Nusser et al., 1995)~~. Briefly, the rabbit and guinea pig antibodies to HCN1 were diluted in TBS containing 2% NGS and 0.05% Triton X-100 at final concentrations of 2-4 µg/ml and 1.4 µg/ml, respectively. Sections for fluorescence double-labeling experiments were further incubated in the mixture of Alexa-594 conjugated goat anti-rabbit IgG (1:500, Molecular Probes, Leiden, The Netherlands; diluted in TBS containing 2% NGS) and biotinylated goat anti-guinea pig IgG (Vector Laboratories, Burlingame, CA; diluted 1:50) for 3 hours. Following several washes, the sections were incubated in avidin-biotinylated HRP complex (ABC, Vector Labs.) for 2 hours followed by a tiramid-oregon green (Molecular Probes) reaction as described by the manufacturer. After several washes in buffer, the sections were mounted on slides in Vectashield (Vector Labs.). Sections for immunoperoxidase reactions were incubated in biotinylated goat anti-rabbit or goat anti-guinea pig IgGs (Vector Labs.; diluted 1:50 in TBS containing 2% NGS) for 3 hours, followed by several washes, and an incubation in ABC for 2 hours. The enzyme reaction was revealed by 3'3-diaminobenzidine tetrahydrochloride (0.05 %) as chromogen and 0.01% H_2O_2 as oxidant. Sections for immunogold reaction were incubated in goat anti-rabbit or goat anti-guinea pig IgGs coupled to 0.8 nm gold particles (Aurion Immunoresearch, Wageningen, The Netherlands; diluted 1:50 in TBS containing 2% NGS). The UltraSmall gold particles were silver enhanced using R-Gent SE-LM Silver kit as described by the manufacturer (Aurion). For light microscopy, sections were mounted on gelatin-coated slides, dried, dehydrated and embedded in DePeX mounting medium (Electron Microscopy Sciences, Washington, PA). Sections for electron microscopy were postfixed with 0.5-1% OsO_4, contrasted in 1% uranyl acetate, dehydrated in graded alcohol series and embedded into epoxy resin (Durcupan, Fluka, Buchs, Switzerland). No specific immunoreactivity could be detected when either the primary or the secondary or both antibodies were omitted and the sections were treated with the silver kit.

Quantitative analysis of the immunogold reactions

As the light microscopic distribution and the qualitative pattern of HCN1 immunogold distribution was practically the same in layer V, hippocampal CA1 and subicular pyramidal cells, we have chosen subicular pyramidal cells to quantitatively evaluate the relative densities of HCN1 in distinct subcellular compartments. The reason for this was that the strongest immunolabeling was observed in the subiculum, allowing the achievement of the highest signal to noise ratio. The highest possible signal is essential for revealing all subcellular compartments with significant amounts of immunoreactive HCN1. The disadvantage of choosing subicular compared to CA1 pyramidal cells is that the pyramidal cell bodies are not arranged in a well-defined layer in the subiculum. Thus, the distance of a dendrite from the soma cannot be easily determined from its location. Consequently, we focused our attention to the following distal and proximal subcellular compartments: distal dendritic plasma membranes; dendritic cytoplasm; distal spine membranes; spine cytoplasm; proximal dendritic plasma membranes; dendritic cytoplasm; proximal spine membranes; spine cytoplasm; somatic plasma membranes; somatic cytoplasm. We calculated the nonspecific immunoparticle density over pyramidal cell nuclei, as this compartment should not contain any HCN1. Samples representing proximal dendrites and spines were taken from regions adjacent to the somata of pyramidal cells located close to the alveus (deep layers). Samples representing the distal part of apical dendrites and spines were taken from the stratum moleculare. Electron micrographs were taken within the same ultrathin section from randomly selected fields in stratum moleculare (30.2±7.5 images per animal) and in deep subicular layers (27.5±9 images per animal). Parts of a pyramidal cell soma were reconstructed from an average of 23 micrographs in 2-4 serial sections. A total of 31 pyramidal cell somata is included in the study. Special care was taken that the ultrathin sections contained tissue from the same depth and reactions were only compared within the same depth. Reactions, obtained with the rabbit antibody, at 3, 4.5 and 6 μm depths were analyzed. Both specific and nonspecific immunoparticle density decreased as a function of depth into the tissue. Thus, we concluded that specific immunoparticle densities could only be compared within the same depth of the tissue. The highest signal to noise ratio was found at 3 μm depth from the surface, therefore all data in the manuscript is acquired at this depth. For reactions obtained with the guinea pig antibody, all measurements were made at the surface of the tissue (within the first μm), because nonspecific labeling density was virtually zero over the nuclei already at this depth.

In each electron micrograph, dendritic shafts, spines and pyramidal somata were identified and gold particles were counted in their cytoplasm as well as on the plasma membranes. Pyramidal cell dendrites were identified from the lack of asymmetrical synapses on the shaft, they may receive symmetrical synapses, and they usually contained mitochondria. Spines were identified as receiving asymmetrical synapses and from the lack of mitochondria. Both labeled and unlabeled profiles were included in the analysis. We have measured the distances of gold particles from the plasma membranes (from the middle of the membrane to the middle of the particle) and analyzed their distribution. As shown in **figure 6. 6A**, a Gaussian distribution provided an adequate fit to the data with a peak location of 24 nm from the membrane and an SD of 11.5 nm. We have considered a gold particle to be associated with the plasma membrane if it was within 46 nm from the cytoplasmic side of the membrane (± 2 x SD around the mean), resulting in an effective membrane width of 46 nm. The immunoparticle density could be calculated in particle / effective membrane area in an EM picture (in particle / μm^2) over all plasma membrane compartments and could be statistically compared to the nonspecific labeling densities (also given in particle / μm^2) with the paired t-test. Membrane lengths (in μm) and areas (in μm^2) were measured with Scion Image 4.0.2 (2000 Scion Corporation, Bethesda, USA). Immunoparticle densities for somatic, dendritic and spine cytoplasm were also calculated in particle / area (in particle / μm^2) and were statistically compared to the nonspecific labeling density with the paired t-test. For those plasma membrane compartments that were found to contain significant amounts of immunoreactive HCN1 (**Fig. 6. 6B** and **C**), we also calculated immunoparticle densities in particle per cut membrane length following nonspecific labeling subtraction (**Fig. 6. 6B** and **C** insets). Data are given as mean ± SD.

4. Identified sources and targets of slow inhibition in the neocortex

SUMMARY

Inhibition in the cerebral cortex is comprised of two types of inhibitory postsynaptic potentials. Fast inhibition is mediated by ionotropic $GABA_A$ receptors and slow inhibition is due to metabotropic $GABA_B$ receptors. Several neuron classes were found to elicit inhibitory postsynaptic potentials through $GABA_A$ receptors, but possible distinct sources of slow inhibition remained unknown. Here we identify a class of GABAergic interneuron, the neurogliaform cells, that in contrast to other GABA-releasing cells, elicited combined $GABA_A$ and $GABA_B$ receptor mediated responses with single action potentials and predominantly targeted dendritic spines of pyramidal neurons. Slow inhibition evoked by a distinct interneuron in spatially restricted postsynaptic compartments could locally and selectively modulate cortical excitability.

INTRODUCTION

Gamma aminobutyric acid is the major inhibitory transmitter in the cerebral cortex (Krnjevic and Schwartz, 1967)~~(Krnjevic and Schwartz, 1967)~~. Extracellular stimulation of afferent cortical fibers elicits biphasic IPSPs in cortical cells. The early phase is due to the activation of $GABA_A$ receptors producing a Cl^- conductance, the late phase is mediated by K^+ channels linked to $GABA_B$ receptors through G-proteins (Dutar and Nicoll, 1988; Mody et al., 1994; Misgeld et al., 1995; Barnard et al., 1998; Bowery et al., 2002)~~Dutar and Nicoll, 1988; Mody et al., 1994; Misgeld et al., 1995; Barnard et al., 1998; Bowery et al., 2002)~~. Although dual recordings revealed several classes of interneurons evoking fast, $GABA_A$ receptor mediated responses in the postsynaptic cells, it is not clear whether distinct groups of inhibitory cells are responsible for activating $GABA_A$ and $GABA_B$ receptors. GABAergic neurones terminate on separate subcellular domains of target cells, (Freund and Buzsaki, 1996; Somogyi et al., 1998a)~~(Freund and Buzsaki, 1996; Somogyi et al., 1998a)~~ and several studies suggested that dendritic inhibition is mediated by $GABA_B$ receptors and possibly by a discrete group of interneurons (Lacaille and Schwartzkroin, 1988; Benardo, 1994)~~(Lacaille and Schwartzkroin, 1988; Benardo, 1994)~~. IPSPs with similar kinetics to $GABA_B$ receptor mediated responses were produced by interneurons

possibly targeting the dendritic regions in the hippocampus (Lacaille and Schwartzkroin, 1988)~~(Lacaille and Schwartzkroin, 1988)~~, but other experiments provided evidence for pure $GABA_A$ responses evoked on dendrites (Buhl et al., 1994; Miles et al., 1996; Thomson et al., 1996; Gupta et al., 2000)~~(Buhl et al., 1994; Miles et al., 1996; Thomson et al., 1996; Gupta et al., 2000)~~. Moreover, it was suggested that repetitive firing of interneurons and/or cooperation of several interneurons is necessary for the activation of $GABA_B$ receptors (Mody et al., 1994; Thomson et al., 1996; Thomson and Destexhe, 1999)~~(Mody et al., 1994; Thomson et al., 1996; Thomson and Destexhe, 1999)~~ possibly by producing extracellular accumulation of GABA to levels sufficient to activate extrasynaptic receptors (Dutar and Nicoll, 1988; Isaacson et al., 1993; Destexhe and Sejnowski, 1995; Thomson et al., 1996)~~(Dutar and Nicoll, 1988; Isaacson et al., 1993; Destexhe and Sejnowski, 1995; Thomson et al., 1996)~~. Here we report that single action potentials evoked in a class of cortical interneuron are sufficient to elicit combined $GABA_A$ and $GABA_B$ receptor mediated responses and determine the site of postsynaptic action as dendritic spines and shafts.

RESULTS

Whole cell recordings with biocytin filling from synaptically coupled pairs of three types of presynaptic interneuron and postsynaptic pyramidal cells combined with correlated light and electron microscopy were performed (Tamas et al., 2000).~~(Tamas et al., 2000).~~ Studies on the localization of $GABA_B$ receptors indicated a gradient-like immunoreactivity for $GABA_B$ receptors with stronger labelling in the upper layers (Lopez-Bendito et al., 2002)~~(Lopez-Bendito et al., 2002)~~, therefore we tried to identify the sources of slow inhibition in layers 2-3 of rat somatosensory cortex. Neurogliaform cells (NGFCs, n = 67) were identified based on late spiking firing pattern **(Fig. 4. 1A, D)** and their axonal and dendritic morphology **(Fig. 4. 2)** (Cajal, 1904; Valverde, 1971; Jones, 1975; Hestrin and Armstrong, 1996; Kawaguchi and Kubota, 1996) ~~(Cajal, 1904; Valverde, 1971; Jones, 1975; Hestrin and Armstrong, 1996; Kawaguchi and Kubota, 1997) (Fig. 1a, d)~~. Basket cells (n = 19) showed fast spiking firing pattern, received depressing unitary EPSPs arriving from pyramidal cells (n = 5), immunoreactivity for parvalbumin (n = 4 out of 4 tested) and they preferentially innervated postsynaptic somata (31 %), dendritic shafts (66 %) and occasionally spines (3 %). Bitufted cells (n = 15) responded to depolarizing current pulses with a so-called low-threshold spiking firing

pattern (Kawaguchi and Kubota, 1997; Reyes et al., 1998), received facilitating EPSPs from neighboring pyramidal cells (n = 3), placed their synapses onto dendritic shafts and spines (74 %; 26 %; n = 45), and, when tested, contained somatostatin (n = 4). Postsynaptic potentials in pyramidal neurons elicited by NGFCs showed slower ($p < 0.001$, Mann-Whitney test) 10-90 % rise times (23.4 ± 9.87 ms, n = 38) when compared to IPSPs due to basket (5.8 ± 2.0 ms, n = 19) or bitufted cell (6.5 ± 1.7 ms, n = 15) activation (**Fig. 4. 1B**). The decay of NGFC to pyramid IPSPs could not be fitted with single or double exponential functions, therefore we have measured the half-width of IPSPs for statistical comparison and found that NGFC to pyramid IPSPs were significantly longer ($p < 0.001$; 183.9 ± 82.5 ms, 61.3 ± 16.3 ms, and 58.9 ± 17.9 ms for NGFC, basket and bitufted to pyramid connections, respectively). Repeating the experiments holding the postsynaptic pyramidal cells in voltage clamp mode confirmed the conclusions of voltage recordings (**Fig. 4. 1C**).

Somata of NGFCs were small (10-15 μm in diameter) and often spherical (**Fig. 4. 2a**). Thin dendrites radiated out from soma, branched once or twice and usually formed a spherical dendritic field around the soma. Dendrites were occasionally beaded and aspiny, or only rarely beared spines (**Fig. 4. 2A**). The axon was extremely thin and arised from any part of the soma. Following the first few brancing of the main axon, thin secondary-tertiary axon branches curved back toward the soma, and this was characteristic for most of the NGFCs (Fig. **4. 2A**). The thin NGFC axons were densely packed with very small boutons (0.4 ± 0.1 μm), compared to the large axon terminals (1.2 ± 0.3 μm) of basket cells (**Fig. 4. 2B**). NGFC axons formed a very dense, highly ramified axon arborization around the soma (**Fig. 4. 2C**) and sent occasionally collaterals into deeper layers.

Random electron microscopic sampling of postsynaptic targets showed that NGFCs predominantly innervated dendritic spines (71 %) and shafts (29 %, n = 65 target profiles; **Fig. 4. 2D**). Three-dimensional light microscopic mapping of NGFC to pyramid connections (n = 8) confirmed the results of random electron microscopic analysis of targets postsynaptic to NGFCs and predicted synapses on dendritic spines and shafts of pyramidal cells at distances 62 ± 28 μm from the somata. Full electron microscopic analysis of all light microscopically mapped synapses was performed on a randomly selected pair and revealed one synapse on a dendritic

Fig.4. 1. **Electrophysiology and anatomy of neurogliaform cell to pyramidal cell connections.**

A, Response of a neurogliaform cell to hyperpolarizing (top) and depolarizing (middle and bottom) current steps. **B, C**, A single action potential (blue) elicited in a neurogliaform cell evokes ipsps (black) in the postsynaptic pyramidal cells (average of n = 54 paired recordings). Superimposed traces comparing fast and slow IPSPs (B) and IPSCs (C) from basket cell to pyramid (green, average of n = 19 pairs) and bitufted cell to pyramid (red, average of n = 15 pairs) with the neurogliaform to pyramid connections at –50 mV membrane potential. The expanded timescale of the bottom panels reveals the differences in activation kinetics. **D**, Reconstruction of a neurogliaform cell (soma and dendrites, blue, axon red) to pyramid (soma and dendrites, black, axon green) connection. Inset, number and position of electron microscopically verified synapses mediating the connection. Cortical layers are inicated on the right. **E**, Serial electron microscopic sections of a synaptic junction (arrow, corresponding to number 1 on panel D)established by the axon of the neurogliaform cell (a) targeting the base of a spine (s) emerging from a dendritic shaft (d) of the pyramidal cell.

Fig 4.1

spine neck, three on spine heads and one on a dendritic shaft 63 μm ± 27 μm (25-92 μm) from the soma (**Fig. 4. 1D-E)**. Pharmacological analysis of NGFC to pyramid interactions revealed that these IPSPs were composed of two components (n = 18, Fig. **4. 3A-B**). The early component could be blocked bybicuculline (10 μM, n = 10) indicating the involvement of $GABA_A$ receptors in the transmission (**Fig. 4. 3A**). Bicuculline blockade alone never abolished the response completely and revealed a residual slow component of neurogliaform IPSPs. This late component could be blocked by further addition of the $GABA_B$ receptor antagonist CGP35348 (60 μM) indicating the involvement of $GABA_B$ receptors in the postsynaptic response. The presence of a postsynaptic $GABA_B$ receptor mediated slow component was confirmed by experiments in which the decay of NGFC to pyramid IPSPs was reversibly shortened by CGP35348 (n = 8, **Fig. 4. 3B**). Furthermore, the early component was absent at -72 ± 1 mV (n = 6), the calculated reversal potential for chloride ions (**Fig. 4. 3C**), therefore chloride passage through $GABA_A$ receptors was responsible for the early phase in agreement with the bicuculline blockade.

The compound IPSPs were highly sensitive to the firing rate of the presynaptic neurones and this could explain why the sources for slow inhibition remained obscure up to date. Temporal dynamics of the neurogliaform IPSPs were first tested by activating the presynaptic cells with single action potentials delivered at various intervals and stable amplitude of postsynaptic responses could only be achieved if the interval between presynaptic spikes was more than 1.5 minutes. Accordingly, all single action potential evoked responses for kinetics, pharmacology and reversal potentials detailed above were collected at especially low presynaptic firing rates (one spike in 100-120 s). When activating the presynaptic NGFCs with trains of action potentials at 40 Hz, the amplitude of postsynaptic responses decreased rapidly (**Fig. 4. 3D**). Even at a train interval of 4 minutes (n = 7), postsynaptic responses showed rapid decrease in amplitude

Figure 4.2. **Anatomical identification of neurogliaform cells.**

A, Light micrograph of a biocytin filled neurogliaform cell in layer 2. After the first two-three branch points of the main axon (arrowhead), secondary-tertiary axon branches (asterisks) curved back toward the soma, and this was characteristic for most of the neurogliaform cells. **B**, High magnification light micrograph of biocytin filled a NGFC axon (right) and basket (left) axon collaterals. The thin NGFC axon is densely packed with very small boutons, compared to the large axon terminals of basket cells. **C**, Reconstruction of a neurogliaform cells (somata and dendrites red, axons blue). Cortical layers are inicated on the right. **D**, Two expamles of random electron microscopic samples of targets postsynaptic to NGFCs. Up, labeled neurogliaform axons (a) form a synapses (arrows) on a on a spine head (s) and on a dendrite (d; down) at the base of a spine (s, left). Asterisks mark asymmetrical synapses established by unidentified terminals (t).

Fig 4.2

resulting in complete loss of response after five to eight presynaptic spike trains. After total exhaustion, recovery of IPSP amplitude was tested with a single presynaptic spike in every 15 minutes and showed recovery in all cases. The recovery was initially detectable after 15-45 minutes and reached 31-79 % of control amplitude as measured after 90 minutes of exhaustion indicating that the synapses remained functional.

DISCUSSION

Our results provide evidence that slow, $GABA_B$ receptor-mediated IPSPs arrive from unitary sources in cortical networks. We identify the first cell type, NGFCs, which consistently recruit postsynaptic $GABA_B$ receptors in addition to $GABA_A$ channels. Synapses of neurogliaform cells appear specialized for sparse temporal operation tuned for long-lasting metabotropic effects. Although it was suggested that in some interneuron to pyramidal cell connections, repeated presynaptic activation might be necessary to recruit slow inhibition (Thomson et al., 1996; Thomson and Destexhe, 1999), single action potentials at very low firing rates are sufficient to elicit the metabotropic $GABA_B$ component. GABA uptake mechanisms powerfully remove the transmitter from the extracellular space within a distance restricted to about a micrometer from the release sites (Overstreet et al., 2000), therefore our results suggest that postsynaptic $GABA_B$ receptors could be spatially associated with the synapses formed by NGFCs. Electron microscopic studies could reveal extrasynaptically placed $GABA_B$ receptors on dendritic spines and shafts (Fritschy et al., 1999; Kulik et al., 2002; Lopez-Bendito et al., 2002), but a possible synaptic enrichment of these receptors remains to be determined. We show that action of NGFCs

Fig. 4. 3. **Pharmacology of neurogliaform to pyramidal cell connections.**

Traces show averages ± s.e. (gray) of several pairs. A, The initial component of control IPSPs (n = 10) elicited by single presynaptic action potentials (top) was blocked by bicuculline (10 μM) and the late phase of IPSP was abolished by the subsequent addition of CGP35348 (60 μM). The IPSPs showed recovery after 30 mins of washout. B, The decay of the IPSPs (n = 8) evoked by single spikes in neurogliaform cells (top) could be shortened by application of CGP35348 (60 μM) and this effect could be partially reversed by returning to the control solution. Superimposed traces are shown normalized to the amplitude of control IPSPs (bottom). C, Voltage dependency of the unitary neurogliaform to pyramid IPSPs (n = 6) recorded at –50 and –72 mV membrane potential. The early phase shows a reversal potential of –72 mV, but the late phase remains identifiable. d, Rapid, use-dependent exhaustion of NGFC to pyramid connections demonstrated by a triple recording with a single presynaptic and two postsynaptic cells. Top, the first five consecutive postsynaptic responses (single sweeps) to presynaptic spike trains elicited once in four minutes. Bottom, single postsynaptic responses to a presynaptic spike after an inactive period of 30 minutes.

is predominantly targeted to site of the anatomically defined biochemical and functional compartments of pyramidal cells, the dendritic spines. The slow rise times of NGFC to pyramidal cell IPSPs and IPSCs might also support spines as targets reflecting the filtering effect of the spine necks but, alternatively, $GABA_A$ receptor subunit composition could also influence activation kinetics (Pearce, 1993; Banks et al., 1998). Although we cannot rule out that neurogliaform synapses on dendritic shafts and spines act through different receptors, data from the cerebellum suggest that $GABA_B$ receptors could be placed on spines (Fritschy et al., 1999; Lopez-Bendito et al., 2002). Spines also receive the majority of excitatory input and simulations showed that if inhibitory synapses found on cortical spines are effective, then they should be mediated through $GABA_B$ receptors providing powerful hyperpolarizing inhibition reducing the excitatory synaptic potentials on the same spine (Qian and Sejnowski, 1990). In addition to hyperpolarizating inhibitory effects, the diffusion barrier provided by the targeted postsynaptic spines can locally enhance metabotropic changes following $GABA_B$ receptor activation, therefore even sparse temporal operation of NGFCs could result in sustained modulation of excitability.

5. β and γ frequency synchronization by dendritic GABAergic synapses and gap junctions in a network of cortical interneurons

SUMMARY

Distinct interneuron populations innervate perisomatic and dendritic regions of cortical cells. Perisomatically terminating GABAergic inputs are effective in timing postsynaptic action potentials, and basket cells synchronize each other via gap junctions combined with neighboring GABAergic synapses. The function of dendritic GABAergic synapses in cortical rhythmicity and their interaction with electrical synapses is not understood.

Using multiple whole cell recordings in layers 2-3 of rat somatosensory cortex combined with light and electron microscopic determination of sites of interaction, we studied the interactions between regular spiking nonpyramidal cells (RSNPCs). Random samples of unlabeled postsynaptic targets showed that RSNPCs placed GABAergic synapses onto dendritic spines (53±12 %) and shafts (45±10 %) and occasionally somata (2±4 %). GABAergic interactions between RSNPCs were mediated by 4±2 axo-dendritic synapses and phased postsynaptic activity at beta frequency, but were ineffective in phasing at gamma rhythm. Electrical interactions of RSNPCs were transmitted via 2-8 gap junctions between dendritic shafts and/or spines. Elicited at beta and gamma frequencies, gap junctional potentials timed postsynaptic spikes with a phase lag, however strong electrical coupling could synchronize pre- and postsynaptic activity. Combined unitary GABAergic and gap junctional connections of moderate strength produced beta and gamma frequency synchronization of the coupled RSNPCs.

Our results provide evidence that dendritic GABAergic and/or gap junctional mechanisms effectively transmit suprathreshold information in a population of interneurons at behaviorally relevant frequencies. A coherent network of GABAergic cells targeting the dendrites could provide a pathway for rhythmic activity spatially segregated from perisomatic mechanisms of synchronization.

INTRODUCTION

Oscillatory activity in different frequency bands occurs in the EEG during various behavioral states in mammals including humans (Niedermeyer and Lopes da Silva, 1993). Particular cortical rhythms are clearly stimulus and task-specific (Buzsaki et al., 1983; Singer, 1993; Steriade et al., 1993). Gamma band EEG activity have been observed in the neocortex in vivo associated with a number of cognitive processes, such as perception or attentional mechanisms (Steriade et al., 1993; Lisman and Idiart, 1995; Mainen and Sejnowski, 1995; Singer and Gray, 1995; Buzsaki, 1996; Jefferys et al., 1996; Steriade et al., 1996) and beta rhythms at 20 Hz are related to voluntarily controlled sensorimotor actions (Salmelin et al., 1995). Cortical GABAergic mechanisms have been implicated in governing population activity (Lytton and Sejnowski, 1991; Buzsaki and Chrobak, 1995; Cobb et al., 1995; Traub et al., 1996; Fisahn et al., 1998). Electrical synapses play a role in neuronal synchrony (Christie et al., 1989; Draguhn et al., 1998; Mann-Metzer and Yarom, 1999) and gap junctional coupling can promote synchronous activity in connections of cortical interneurons (Galarreta and Hestrin, 1999; Gibson et al., 1999; Koos and Tepper, 1999; Tamas et al., 2000; Venance et al., 2000). The precise spatiotemporal cooperation of gap junctional coupling with GABAergic synapses between basket cells further enhances populational coherence (Tamas et al., 2000).

GABAergic cells subdivide the surface of their target neurons (Somogyi et al., 1998a), but most experiments addressing synchronization either did not examine the location of the inputs or were focused on perisomatic mechanisms (Cobb et al., 1995; Gupta et al., 2000; Tamas et al., 2000). Recent evidence suggests that a delicate balance of perisomatic and dendritic inhibition is essential in maintaining normal cortical rhythmogenesis since a deficit in dendritic inhibition could reduce seizure threshold, whereas enhanced somatic inhibition would prevent the

Figure 5. 1. **Identification of RSNPCs and modulation of their firing by presynaptic beta and gamma frequency activity of layer 2/3 pyramidal cells.**

A, Response of a RSNPC to a depolarizing (Aa, 180 pA) and hyperpolarizing (Ab, -100 pA) current pulse. *B*, Biocytin filled axon terminals (t) of RSNPCs formed synapses (arrows) with unlabeled dendritic shafts (Ba, d) and spines (Bb, s). *Ca*, Pyramidal cell firing at 19 Hz (top) elicited EPSPs showing marked activity-dependent depression in a postsynaptic RSNPC (middle). Subsequently, the postsynaptic cell was tonically depolarized to fire at a frequency of ~ 4 Hz (bottom, 50 consecutive superimposed sweeps). *Cb*, Firing probability plot of the postsynaptic RSNPC during a representative presynaptic action potential cycle shows that only the first three cycles were effective in phasing postsynaptic activity at beta frequency.

Fig 5.1

continuous occurrence of epileptiform activity (Cossart et al., 2001). A particular subcellular domain of GABAergic and/or electrical communication might result in compartmental interaction of synaptic and voltage gated conductances, resulting in the domain specific processing of sub- and suprathreshold operations. In this work we identified a population of neocortical interneurons with dendritic target preference, which forms a network interacting via gap junctions, and GABAergic synapses. Neurons of this network are capable of engaging coherent activity and can be activated by local pyramidal cells at beta and gamma frequencies.

RESULTS

Several hundred simultaneous dual, triple and quadruple recordings of neurons in layers 2-3 of rat somatosensory cortex provided 28 regular spiking nonpyramidal cell (RSNPC) to RSNPC connections and 12 pyramidal cell (PC) to RSNPC connections. RSNPCs were identified based on their physiological and anatomical properties (Cauli et al., 1997; Kawaguchi and Kubota, 1997; Cauli et al., 2000). Similar to RSNPCs identified earlier they responded to long (800 ms) depolarizing current pulses with a regular spiking firing pattern showing first to second spike amplitude reduction of 23 ± 11 % and input resistance of 375 ± 117 MΩ (**Fig. 5. 1A**). Local pyramidal cells elicited unitary EPSPs in RSNPCs with paired pulse depression (n = 12; amplitude of the first response: 1.24 ± 1.25 mV; paired pulse ratio: 56 ± 14 % (Porter et al.,

Figure 5. 2. **Dendritic GABAergic synapses can phase somatic action potential generation in a RSNPC to RSNPC connection.**

Data acquired from the pre- and postsynaptic cells are presented in gray and black, respectively. *Aa*, Repetitive presynaptic firing at 19 Hz (top) resulted in the summation of unitary IPSPs followed by the stabilization of their amplitude in the postsynaptic cell (middle). When tonically depolarizing to fire, the postsynaptic RSNPC became effectively entrained with a phase-lag ~ 41 ms throughout the entire duration of presynaptic activity (bottom, 50 consecutive sweeps). *Ab*, Distribution of postsynaptic firing probability during a representative presynaptic action potential cycle. *Ba*, Repeating the experiment shown in A with 37 Hz presynaptic activation (top), resulted in early summation and subsequent stabilization of IPSP amplitude (middle). GABAergic synapses between RSNPCs were not effective in phasing postsynaptic firing at gamma frequency as shown by 50 consecutive superimposed sweeps (Ba, bottom) and average firing probability distribution during a presynaptic cycle (Bb). *C*, Distribution of GABAergic input on the dendritic tree of the postsynaptic RSNPC (black). The axon of the presynaptic cell (gray) innervated secondary and tertiary dendrites (arrows) as detected by light microscopy. D, Dendrogram representing the innervated dendritic segments of the postsynaptic cell and three-dimensional distances of synapses (arrows).

Fig 5.2 +legend

1998). The dendrites of RSNPCs originated from the two poles of their elongated somata (**Fig. 5. 2C, 3B-C, 4C**) and were sparsely spiny (**Fig. 5. 3E-F**). The axons formed a dense cloud around the dendritic tree and sent a loose bundle of radial branches spanning all layers of the cortex (**Fig. 5. 3B**). High order axonal branches of RSNPCs run radially and branched rectangularly (**Fig. 5. 2C, 4C**). Electron microscopic random samples of unlabeled postsynaptic targets (n = 267) taken from layers 2-5 showed that RSNPCs (n = 10) innervated dendritic spines (53 ± 12 %) and shafts (45 ± 10 %) and occasionally somata (2 ± 4 %, **Fig. 5. 1B**). Detailed analysis of serial sections revealed that only 44 ± 21 % of postsynaptic targets identified as dendritic spines received asymmetrical synapses.

Rhythmic activation of RSNPCs by local PCs was tested in six pairs at beta and gamma frequencies (19 and 37 Hz, respectively). Presynaptic PC firing at both frequencies resulted in use-dependent depression of postsynaptic unitary EPSPs in all RSNPCs (**Fig. 5. 1Ca**).

Figure 5. 3. **Gap junctional connections between RSNPCs.**

A-H, Synchronization of a pair of RSNPCs by strong gap junctional coupling. *Aa*, Electrical coupling produces gap junctional potentials of relatively stable amplitude (middle) in response to presynaptic trains of action potentials delivered at 37 Hz (top). The scattergram represents the timing of individual action potentials in 50 consecutive trials during tonic depolarization of the postsynaptic cell. Robust gap junctional coupling was highly potent in synchronizing pre- and postsynaptic activity as shown by the overlay of the 50 trials (bottom). *Ab*, Distribution of postsynaptic action potentials relative to a presynaptic cycle. B-H, Anatomical correlates of the electrical interaction shown in panel A. *B*, Reconstructions of RSNPC 1 (soma and dendrites: gray, axon: black) and RSNPC 2 (soma and dendrites: black, axon: gray) cells. Cortical layers are indicated in the middle (I-V). *C*, Relative arrangement of somata and dendrites of the coupled cells. Electron microscopically identified gap junctions (arrowheads) mediating the interaction between the coupled cells were found on dendrites. *D*, Dendrograms representing three-dimensional dendritic distances of gap junctions (arrowheads). *E-H*, Examples of the 8 electron microscopically identified gap junctions (arrowheads) between the RSNPCs. Insets show the junctional regions at higher magnification. *E*, Dendritic spines (s) establish a gap junction between RSNPC 1 (left) and RSNPC 2 (right; d, parent dendritic shafts). *F*, Gap junction between a dendritic spine (s) of RSNPC 1 and a dendritic shaft (d) of RSNPC 2. *G-H*, Dendritic shafts of RSNPC1 and 2 (d) form gap junctions. Note the parallel membrane appositions with widened extracellular space of 21-25 nm (*) adjacent to both dendro-dendritic gap junctions. Synaptic junctions are indicated (arrows) between unlabeled terminals (t) and the dendrites of RSNPC 1. *I*, Electrical coupling between RSNPCs entrained postsynaptic firing with a phase lag in most pairs examined. *Ia*, Presynaptic action potentials at 37 Hz (top) elicited gap junctional potentials of moderate amplitude in the postsynaptic cell (middle, same scale as in panel Aa). When tonically depolarizing the postsynaptic RSNPC to fire, postsynaptic action potentials became entrained with a phase-lag ~ 6 ms throughout the entire duration of presynaptic activity (50 consecutive sweeps). *Ib*, Distribution of postsynaptic firing probability during a representative presynaptic action potential cycle.

Fig 5. 3

Presynaptic spike trains at beta rhythm increased the mean frequency of ongoing postsynaptic firing to 125 ± 14 % of the control value, respectively (from 4.2 ± 1.4 Hz to 5.3 ± 1.7 Hz; **Fig. 5. 1Ca, 5B**). Beta frequency presynaptic activation entrained postsynaptic firing during the first three presynaptic cycles. During these cycles, postsynaptic firing probability was significantly higher in the first three bins (0 - 22.3 ms) after the preceding presynaptic spike than later (**Fig. 5. 1Cb, 5B**). In parallel with the depression of unitary EPSPs, phasing effectiveness of PCs on RSNPC firing faded during the rest of presynaptic activity (**Fig. 5. 1Cb**). Similar results were obtained at gamma frequency PC activation (**Fig 5. 5B**). When driving the PCs at 37 Hz, the mean firing rate of postsynaptic RSNPCs was accelerated to 132 ± 26 % of the control and entrainment of postsynaptic firing was limited to the first two (n = 3 pairs) or three (n = 3 pairs) presynaptic cycles. During these cycles, postsynaptic firing probability was significantly higher in the second and third bins (7.4 - 22.3 ms) after the preceding presynaptic spike than during the rest of bins (**Fig. 5. 1Cb, 5B**). We identified GABAergic, electrical and combined GABAergic and electrical connections between RSNPCs. In pairs of RSNPCs connected by chemical synapses only (n = 12), light microscopic analysis of six fully visualized cell pairs indicated 4 ± 2 close appositions betweenpresynaptic axons and postsynaptic dendrites at a mean distance of 63 ± 28 μm from the somata (**Fig. 5. 2C-D**). All GABAergic connections were unidirectional between RSNPCs in our sample. Measured at –51 ± 3 mV membrane potential, unitary IPSPs between RSNPCs were 0.54 ± 0.23 mV in amplitude (n = 12). Bicuculline completely abolished the responses (20 μM; n = 3). Repetitive presynaptic firing at 19 and 37 Hz resulted in the summation of postsynaptic unitary IPSPs followed by the stabilization of their amplitude ~ 198 ± 49 and 238 ± 57 % of the amplitude of averaged single events, respectively (n = 6; **Fig. 5. 2Aa, Ba**). Presynaptic spike trains (19 Hz) decreased the mean frequency of spontaneous postsynaptic firing to 79 ± 18 % of the control value (from 4.6 ± 1.9 Hz to 3.6 ± 1.7 Hz). Postsynaptic firing was entrained for the entire duration of presynaptic activation. Postsynaptic firing probability was significantly smaller in the second and third bins (7.4 - 22.3 ms) after the preceding presynaptic spike than during the first, sixth and seventh bins (0 - 7.4 ms and 37.1 – 52 ms) in a cycle (**Fig. 5. 2Ab, 5C**). Gamma frequency presynaptic activation (37 Hz) could decrease the mean postsynaptic discharge rate from 4.7 ± 1.7 Hz to 3.2 ± 1.3 Hz (69 ± 12 %) but was not effective in phasing postsynaptic action potential generation (**Fig. 5. 2B, 5C**).

The second class of RSNPC to RSNPC connections was mediated by electrical synapses (n = 12). Light microscopic mapping in 5 fully recovered pairs detected 3 ± 3 close appositions (range, 2 - 8) exclusively between dendrites at a mean distance of 77 ± 34 µm from the somata **(Fig. 5. 3B-D**). Electron microscopic analysis of the suspected coupling sites was carried out in one cell pair, leading to the identification of eight gap junctions in the connection at dendritic distances of 72 ± 16 µm (cell 1) and 63 ± 36 µm (cell 2) from the somata (**Fig. 5. 3C-H**). Two gap junctions were established between dendritic spines, one between a spine and a dendritic shaft and four gap junctions linked dendritic shafts. Analysis of serial ultrathin sections showed in all four dendritic shaft to dendritic shaft cases that the junctional region was composed of the gap junction and an immediately adjacent patch of membranes running parallel for 0.3 - 0.9 µm at a rigid distance of 21 - 25 nm (**Fig. 5. 3G-H)**. The latter value is characteristic of desmosomes and/or synaptic clefts but the electron opaque reaction end product prevented further identification of junctional components. All electrical connections between RSNPCs were reciprocal. Gap junctional potentials (GJPs) showed a relatively wide range in amplitude (0.07 - 2.42 mV; 0.62 ± 0.74 mV) at –50 ± 3 mV membrane potential and had an average duration of 19.6 ± 8.2 ms, as measured at half amplitude. They followed presynaptic action potentials with a delay of 0.40 ± 0.26 ms, measured as the period spanning the maximal rates of rise of the presynaptic action potential and the GJP, respectively. The average amplitude ratio (coupling coefficient) for GJPs and presynaptic potentials was 0.66 ± 0.83 % (range, 0.04 - 2.58 %) and

Figure 5. 4. **Synchronization of RSNPCs through combined unitary gap junctions and GABAergic synapses targeting the dendritic domain.**

Data obtained from the pre- and postsynaptic cells are presented in gray and black, respectively. *A-B,* Presynaptic action potentials evoked at 19 and 37 Hz (Aa and Ba, top) elicited spikelets followed by short-latency IPSPs in the postsynaptic neuron (middle). Dual coupling of moderate strength synchronized pre- and postsynaptic firing as shown by 50 consecutive trials during tonic depolarization of the postsynaptic cell (Aa and Ba, bottom) and the probability plots of postsynaptic firing during a representative presynaptic cycle (Ab and Bb). C, The route of presynaptic dendrites and axons (grey) to gap junctions (arrowheads) and GABAergic synapses (arrows) on the postsynaptic cell (black). The dendrites and axons of the presynaptic cell are truncated for clarity. *D,* Dendrograms representing the dendritic branches of the two RSNPCs involved in the connections and three-dimensional distances of the sites of interaction. *E-F,* Examples of the 2 electron microscopically identified gap junctions and the 3 GABAergic synapses between the RSNPCs. Insets on the right show the junctional regions at higher magnification. *E,* Gap junction (arrow) between dendritic shafts (d) of the presynaptic (right) and postsynaptic (left) cell. *H,* A terminal (t) of the presynaptic cell establishes a synaptic junction (arrowhead) on a dendritic shaft (d) of the postsynaptic cell.

Fig 5. 4

4.6 ± 3.1 % (range, 2.4 - 10.6 %) when eliciting action potentials and applying long current steps (200 pA, 300 ms duration) in the first neuron to elicit a response in the second neuron. Coupling strength was similar in both directions and did not show voltage dependence between –80 and –40 mV postsynaptic membrane potential (n = 4). Both amplitudes and kinetics of GJPs remained unchanged during repetitive presynaptic firing (**Fig. 5. 3Aa, Ia**). The effect on unitary GJPs on postsynaptic suprathreshold activity was investigated at 19 and 37 Hz in 6 connections. For a given pair, timing of postsynaptic firing was similar at both frequencies tested and members of a pair phased one another with similar efficacy regardless of the direction. In four out of six pairs, 19 Hz presynaptic activation accelerated the mean firing rate of postsynaptic RSNPCs to 120 ± 10 % of the control. Postsynaptic firing probability was significantly higher in the first two bins (0 – 14.9 ms) after the preceding presynaptic spike than during the last three bins (29.7 – 52 ms) of a cycle (**Fig. 5. 5D**). GJPs arriving at gamma frequency increased ongoing postsynaptic firing and firing probability was significantly higher in the second bin (3.9 – 7.7 ms after the presynaptic spike) than in the rest of bins in a cycle (**Fig 5. 3I, 5D**). In the two pairs with the highest coupling ratios and numbers of gap junctions, GJPs synchronized pre- and postsynaptic firing at beta and gamma frequencies with no apparent phase lag (bin width, 3.9 ms) and a relatively narrow temporal scatter of action potentials (**Fig. 5. 3A**).

Six RSNPC to RSNPC connections were mediated by combined GJPs and IPSPs. The GABAergic component of all dual electrical and chemical connections was unidirectional. Light microscopic mapping of three fully recovered pairs revealed that gap junctions as well as chemical synapses were located in the dendritic domain of the postsynaptic cells at a mean distance of 59 ± 21 and 75 ± 18 μm from the somata, respectively. Detailed electron microscopic analysis of one pair confirmed such arrangement of connections and identified two gap junctions

Figure 5. 5. **Differential entrainment of suprathreshold activity by inputs targeting RSNPCs.**

A, Representative presynaptic cycles at beta (19 Hz) and gamma (37 Hz) frequency. *B-E*, Firing probability plots of postsynaptic RSNPCs during representative presynaptic action potential cycles shown in panel A when EPSPs (*B*, n = 6), IPSPs (*C*, n = 5), gap junctions (*D*, n = 4) and dual electrical and GABAergic synapses (*E*, n = 6) mediated unitary interactions. In pyramid-to-RSNPC connections only the first two presynaptic cycles entrained postsynaptic firing in all pairs, the rest of the cycles are not shown (see Fig. 1Cb). The two electrical only connections with the highest coupling ratios and numbers of gap junctions are not presented in this figure (see Results and Fig. 3A-H). *F*, Cluster analysis of the data presented in panels B-E. Controls, connections mediated by IPSPs and combined electrical and GABAergic coupling form distinct groups, interactions through gap junctions only and EPSPs overlap. Dlink/Dmax: linking and maximal Euclidean distances.

5.5

between dendritic shafts (one of them showing rigid widening of extracellular space adjacent to the gap junction) and three GABAergic synapses on dendrites (**Fig. 5. 4C-F**). Postsynaptic responses were composed of GJPs followed by short-latency IPSPs of stable amplitude (**Fig. 5. 4A-B**).

Presynaptic spike trains at 19 and 37 Hz decreased the mean frequency of ongoing postsynaptic firing to 91 ± 11 % and 84 ± 8 % of control values, respectively (from 5.08 ± 1.19 Hz to 3.77 ± 1.13 Hz and from 5.08 ± 1.19 Hz to 3.77 ± 1.13 Hz). Following the onset of presynaptic spike trains postsynaptic firing was instantly synchronized at beta and gamma frequencies, with maximal postsynaptic action potential probability in the first bin (bin widths, 7.4 and 3.9 ms; **Fig. 5. 4Ab, Bb, 5. 5E**). Firing occurred synchronously in the coupled cells during the entire length of presynaptic activation.

Cluster analysis of postsynaptic firing probability in response to beta and gamma frequency presynaptic firing resulted in the clear delineation of controls, connections mediated by IPSPs and combined electrical and GABAergic coupling (**Fig. 5. 5F**). Interactions via moderate gap junctional coupling and EPSPs clustered together (**Fig. 5. 5F**) but the two electrical connections mediated by powerful coupling formed a separate group at both frequencies (not illustrated).

DISCUSSION

We have identified a novel interneuronal network in the cortex interconnected by electrical and GABAergic synapses. RSNPCs form dendritic gap junctions with other RSNPCs and establish GABAergic synapses on the dendritic domain of postsynaptic cells. Electrical, GABAergic, or combined GABAergic and gap junctional signals targeted to the dendrites are capable of timing somatic action potential generation in the network of RSNPCs at behaviorally relevant frequencies.

Interneurons forming the network identified here are distinct of GABAergic cell classes known to form electrically coupled networks in the cortex (Hestrin and Armstrong, 1996; Galarreta and Hestrin, 1999; Tamas et al., 2000; Venance et al., 2000). The regular spiking firing pattern in combination with depressor unitary EPSPs demarcate RSNPCs both from fast spiking cells and from low threshold spiking/bitufted cells (Reyes et al., 1998; Gibson et al., 1999) and

these electrophysiological parameters are similar to those of vasoactive intestinal polypeptide immunoreactive interneurons (Kawaguchi and Kubota, 1996; Cauli et al., 2000). In agreement with earlier results (Kawaguchi and Kubota, 1997; Tamas et al., 1997), we have found that RSNPCs place symmetrical synapses onto dendritic spines and shafts. These results would identify RSNPCs as double bouquet cells (Somogyi and Cowey, 1981; Tamas et al., 1997), but the finding that only less than half of postsynaptic targets identified as dendritic spines received asymmetrical synapses questions the origin of postsynaptic dendritic appendages. Although the synaptology of interneuronal spines are not known, the spines receiving excitatory synapses are most likely originate from pyramidal dendrites; the ones receiving GABAergic innervation only could belong to pyramidal cells as well as GABAergic interneurons. Double bouquet cells target other GABAergic neurons (Tamas et al., 1998) and there are known types of interneuron preferentially innervating other GABAergic cells in the rat (Gulyas et al., 1996; Meskenaite, 1997) and the distinction between these classes are not yet clear. Gap junctions between RSNPCs also connect dendritic shafts and spines and, moreover, GABAergic synapses and gap junctions are placed at similar distances from the soma of RSNPCS. Therefore, similarly to the network of cortical basket cells (Tamas et al., 2000), chemical and electrical synapses target the same subcellular domain of RSNPCs equalizing the time required for postsynaptic signal propagation. Accurate spatial integration could be further promoted by juxtaposition of gap junctions, dendro-dendritic synapses and/or desmosomes found between smooth dendritic shafts in the primate motor cortex (Sloper and Powell, 1978) and between parvalbumin immunoreactive dendrites in the hippocampus (Fukuda and Kosaka, 2000). We found a rigid widening of the extracellular space next to the gap junctions in six out of five contacts between dendritic shafts of RSNPCs, but our method for the visualization of functionally coupled cells did not allow the differentiation of desmosomes and dendro-dendritic synaptic junctions.

We provide evidence that dendritically targeted GABAergic synapses are effective in timing somatic action potentials in the postsynaptic RSNPCs. Mechanisms underlying such phasing are not yet known. GABAergic cell types elicit IPSCs and IPSPs with remarkably different kinetics (Gupta et al., 2000), which could reflect distinct postsynaptic receptor properties (Mody et al., 1994; Draguhn et al., 1998). Currents activated by hyperpolarization (Ih) are present in RSNPCs, but not as prominent as in pyramidal cells and bitufted cells (our unpublished data and (Cauli et al., 2000). Therefore, activation and/or deinactivation of other

voltage gated cation conductances and/or by passive dendritic properties could be the major factors in shaping the relatively fast decay of IPSPs. Dendritic GABAergic synapses between RSNPCs are able to phase postsynaptic cells in the beta frequency band, which is clearly faster than the theta frequency range of rebound activation detected in connections mediated by perisomatically placed GABAergic synapses on pyramidal cells (Cobb et al., 1995) as well as on interneurons (Tamas et al., 2000). The rebound activation might be even faster in vivo, when the input resistance of the cells is likely to be lower due to ongoing background synaptic activity. This could improve phasing between RSNPCs in the gamma frequency band. Theta and beta/gamma rhythms are linked to distinct behaviors (Buzsaki et al., 1983; Singer, 1993; Steriade et al., 1993), and our results suggest that diverse populations of GABAergic cells might be differentially involved in cortical network operations during a particular activity.

Unitary EPSPs could initiate firing in RSNPCs with latencies slightly longer to what has been found in hippocampal interneurons (Fricker and Miles, 2000). The authors measured the timing of spikes elicited from just subthreshold membrane potentials, but we have tested the effectiveness of GJPs and EPSPs (and IPSPs and dual coupling) on spontaneous ongoing firing. The set of voltage gated conductances active at subthreshold membrane potentials and during spontaneous repetitive firing is likely to be different and might explain the discrepancy. The amplitude of GJPs versus EPSPs might also influence the immediacy of spikes after the onset of the postsynaptic potentials by activating different amounts and or populations of voltage gated channels. In addition to spike triggering, suprathreshold activity of RSNPCs can be rhythmically timed with a phase lag by neighboring pyramidal cells in the beta and gamma frequency range.

Strong bidirectional electrical coupling could produce synchronization of RSNPCs, but on average, combined chemical and electrical unitary connections were most effective in synchronizing pre- and postsynaptic firing. In our sample, all GABAergic connections were unidirectional between RSNPCs including the GABAergic component of dual electrical and chemical connections. The implications of unidirectional GABAergic coupling in combination with reciprocal gap junctional connections are not clear. RSNPCs are embedded into a network interconnected by chemical, electrical and dual unitary connections and a particular postsynaptic cell is likely to receive convergent GJPs and IPSPs from some RSNPCs which might be precisely synchronized by dual coupling. This scenario suggests that dual connections would rule the operation of RSNPCs at the network level. Preferred rhythms of RSNPC population oscillations

might be in the beta and probably gamma frequency band set by the timing of rebound activation following unitary IPSPs within the network. Coherent output of RSNPCs could provide a powerful dendritic pathway of rhythmic information processing spatially and temporally segregated from perisomatic mechanisms of synchronization. The cooperation of GABAergic synapses and gap junctions appears to be limited to a single population of interneurons (Galarreta and Hestrin, 1999; Gibson et al., 1999; Tamas et al., 2000; Venance et al., 2000) therefore synchronization might be more prominent within populations than across different interneuron types. This might explain the effectiveness of soma and dendrite targeting interneurons in timing postsynaptic activity of pyramidal cells though a precisely synchronized, robust, but perisomatically and dendritically channeled GABAergic flow of information.

6. Polarized and compartment-dependent distribution of the hyperpolarization-activated channel HCN1 in pyramidal cell dendrites

SUMMARY

The functional role of an ion-channel depends, to a large extent, on its location and density on the surface of nerve cells. A view emerges on the principles governing the precise subcellular distributions of ligand-gated ion-channels, but almost nothing is known about those of voltage-gated channels. Here we used high-resolution immunolocalizations to determine the subcellular distribution of the hyperpolarization-activated and cyclic-nucleotide-gated channel subunit 1 (HCN1). Light microscopy revealed a graded HCN1 immunoreactivity in apical dendrites of hippocampal, subicular, and neocortical layer V pyramidal cells. Quantitative comparison of immunogold densities showed a 60-fold increase from somatic to distal apical dendritic membranes. Distal dendritic shafts had 16-times more HCN1 labeling than proximal dendrites of similar diameters. At the same distance from the soma, the density of HCN1 was significantly higher in dendritic shafts than in spines. Our results reveal the complexity in the cell surface distribution of voltage-gated ion-channels, and predict its role in increasing the computational power of single neurons via subcellular domain and input specific mechanisms.

INTRODUCTION

Ligand- and voltage-gated ion-channels are fundamental building blocks of excitable nerve cells. The molecular diversity of these channels, as revealed in the past decades, contributes to their functional heterogeneity (Hille, 2001). However, it has also been recognized that not only the molecular structure, but also the precise subcellular location and the density of channels are crucial in neuronal communication and integration (Yuste and Tank, 1996; Ottersen and Landsend, 1997; Magee et al., 1998; Petralia et al., 1998; Somogyi et al., 1998b; Conti and Weinberg, 1999; Craig and Boudin, 2001). Recent experiments shed light on some organizational principles of the cell surface expression of ligand-gated ion-channels. For example, high-resolution immunolocalisation studies showed that distinct AMPA-type (Rubio and Wenthold, 1997; Nusser et al., 1998b; Takumi et al., 1999), NMDA-type (Fritschy et al.,

1998; Watanabe et al., 1998; Takumi et al., 1999) glutamate receptor subunits, and $GABA_A$ receptor subunits (Nusser et al., 1996; Fritschy et al., 1998; Nyiri et al., 2001) are selectively targeted to functionally different synapses of a single cell, establishing a presynaptic input-selective distribution of postsynaptic receptors. The amount and density of postsynaptic $GABA_A$ and glutamate receptors are also regulated in a presynaptic input specific manner (Nusser et al., 1997; Nusser et al., 1998b; Nusser et al., 1998c; Takumi et al., 1999). Furthermore, distinct $GABA_A$ receptor subtypes are segregated to synaptic vs. extrasynaptic sites, underlying distinct forms of inhibition in certain cell types (Nusser et al., 1998a).

Much less is known about the cell surface distribution of voltage-gated channels, although its importance in neuronal integration is generally recognized (Yuste and Tank, 1996; Magee, 1998). This is mainly due to the scarcity of high-resolution immunogold localization studies of these channels. A recent study using electron microscopic (EM) immunogold localization of voltage- and Ca-activated K channels (BK) elegantly showed their enrichment in presynaptic active zones of glutamatergic terminals and the lack of labeling on postsynaptic dendrites (Hu et al., 2001). Several experiments mapped voltage-gated channels on the axo-somato-dendritic surface of nerve cells using patch-clamp recordings. This technique is extremely useful as it reveals the location of functional channels. However, small subcellular compartments remain inaccessible with this approach and a differential current density does not necessarily mean distinct densities of channels. Patch-clamp studies suggested uneven subcellular distribution of transient A-type K channels (I_A) (Hoffman et al., 1997), N-type Ca channels (Bischofberger and Schild, 1995; Christie et al., 1995), Na channels (Stuart and Hausser, 1994; Magee and Johnston, 1995), and hyperpolarization-activated (I_h) channels in nerve cells (Schwindt and Crill, 1997; Magee, 1998; Stuart and Spruston, 1998; Magee, 1999a; Tsubokawa et al., 1999; Williams and Stuart, 2000; Berger et al., 2001), but uniform density of Na channel in the axo-somato-dendritic domains of some other cells was also reported (Stuart and Sakmann, 1994; Colbert and Johnston, 1996). However, the differential somato-dendritic distribution of I_A may not necessarily reflect a differential channel distribution, as these channels have been shown to undergo a differential regulation by PKA and PKC across the somato-dendritic surface of hippocampal pyramidal cells (Hoffman and Johnston, 1998). Furthermore, all of these channels/currents have been recorded in large diameter apical dendrites, but their density in small diameter secondary dendrites and in spines remained elusive.

In the present study, we applied EM immunogold localizations of HCN1 to reveal the rules of its cell surface distribution. HCN1 is one of the four known subunits (HCN1-4) of the hyperpolarization-activated and cyclic-nucleotide-gated nonselective cation channels (Santoro et al., 1997; Gauss et al., 1998; Ludwig et al., 1998; Monteggia et al., 2000). The homo- or heteromeric assemblies of these subunits are mainly responsible for the functional diversities of H-current (I_h) (Seifert et al., 1999; Chen et al., 2001). Our results demonstrate that this channel is unevenly distributed in the axo-somato-dendritic surface of pyramidal cells. The distal dendritic shafts had ~60-times higher immunoparticle densities than the somata, while pyramidal cell axons were found to be immunonegative. There was also a ~16-fold difference in the density of HCN1 labeling between small diameter distal and proximal dendrites. Furthermore, distal dendritic shafts had ~4-times higher immunoreactive HCN1 density than spines at the same distance from the soma, revealing a distance- and subcellular domain-specific regulation of the plasma membrane density of HCN1.

RESULTS

Distribution of HCN1 immunoreactivity in the neocortex and the hippocampal formation

The regional, cellular and subcellular distribution of HCN1 was investigated with two polyclonal antibodies (rabbit: HCN1-R; guinea pig: HCN1-Gp) directed against different, non-overlapping parts of the protein (see Methods). The specificity of the rabbit and guinea pig antibodies was verified by immunoblot analysis of crude membrane fractions prepared from adult rat brains (**Fig. 6. 1**). Both antibodies gave a broad immunoreactive band around a molecular mass of 120-kDa, which is consistent with the result of a previous study (Santoro et al., 1997).

The regional and cellular distribution of HCN1 immunostaining as revealed with the two antibodies was practically identical (**Figs. 6. 2** and **3**), demonstrating that the immunolabelling is due to a specific antibody-antigen (HCN1) recognition. In the neocortex, bundles of strongly immunopositive apical dendrites of pyramidal cells appeared at the border of layers III and IV (**Fig. 6. 2**). The labelling intensity of the apical dendrites increased toward layer I, dendritic tufts showing the strongest labelling (**Fig. 6. 2b** and **e**). These dendrites did not contain the calcium binding protein, calbindin D-28K, suggesting that they do not belong to layer II/III pyramidal

cells (data not shown). The large diameter and the appearance of some of these apical dendrites already in layer IV indicate that they belong to layer V pyramidal cells. Higher magnifications

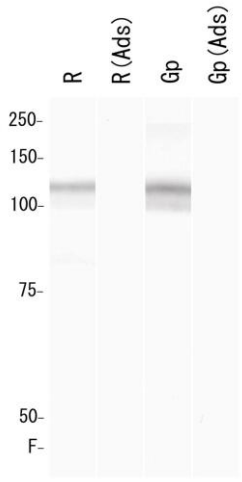

Figure. 6. 1. **Immunoblot analysis of rat brain with HCN1 antibodies.**
Crude membrane preparations from whole rat brains were reacted with HCN1 antibodies raised in a rabbit (R) and a guinea pig (Gp). No immunoreactivity is detected after adsorption of these antibodies with the corresponding antigens (Ads). Molecular mass markers (Bio-Rad, Hercules, CA, USA) are indicated on the left in kDa. F: gel front.

revealed that the strong immunoreactivity of the apical dendrites mainly originated from the strong labelling of the plasma membrane (**Fig. 6. 2c** and **f**). They appeared as tubes with apparently immunonegative cytoplasm surrounded by strongly labelled plasma membranes. Furthermore, dendritic spines emerging from these apical dendrites were also immunopositive in the upper layers (**Figs. 6. 2c, 2f, 3c** and **3d**). These data obtained at the light microscopic (LM) level are consistent with an increased density of HCN1 in the dendrites of layer V pyramidal cell as a function of distance from the soma. Punctate, relatively weak immunostaining of the neuropil was observed in all layers, the somata of nerve cells and the cytoplasm of large diameter dendrites being apparently immunonegative. The staining of the neuropil was stronger with the HCN1-Gp antibody (cf. **Fig. 6. 2b** and **e**), which provided a somewhat stronger staining of all positive structures. This low intensity neuropil labelling may be due to the weak staining of either small diameter secondary/tertiary dendrites, or dendritic spines, or axons/axon terminals, or glial processes, or the combination of the above.

In the hippocampal formation, the most intense immunolabelling for HCN1 was detected in the subiculum, followed by the CA1, CA3 areas, and the dentate gyrus showed the least intense labelling (**Fig. 6. 3a** and **b**). In particular, the stratum moleculare of the subiculum was the strongest subregion of the entire hippocampal formation, followed by the stratum lacunosum-moleculare of the CA1 area (**Fig. 6. 3a** and **b**). The stratum lucidum of the CA3 area was

immunonegative for HCN1, the cell body layers of all hippocampal regions showed moderate labelling of presumable inhibitory axon terminals. In the CA1 area, the intensity of the immunolabelling increased from the stratum pyramidale to the stratum lacunosum-moleculare. This pattern of labelling, as all LM observation of this study, was observed with both immunoperoxidase (**Fig. 6. 2**) and immunofluorescent (**Fig. 6. 3**) methods. Similarly to the neocortex, intense labelling of the plasma membrane of the apical dendrites of CA1 and subicular pyramidal cells was observed at high magnifications. Some hippocampal interneurons also showed intense immunolabelling for HCN1. The identification of the cells and the precise subcellular distribution of HCN1 in these cells were outside the scope of the present study.

As the cell bodies of the CA1 pyramidal cells are nicely arranged in a single well defined layer, the stratum pyramidale, pyramidal cell dendrites and spines in any given segment of the strata radiatum and lacunosum-moleculare are approximately the same distance away from their parent somata. This arrangement allowed us to evaluate possible changes in the immunollabeling intensity as a function of distance from the soma at the light microscopic level. The highest intensity of HCN1 labelling was detected in the stratum lacunosum-moleculare, followed by the stratum radiatum, stratum oriens and the lowest intensity was in the stratum pyramidale. Within stratum radiatum, an increased labelling intensity was apparent toward the stratum lacunosum-moleculare. The most parsimonious explanation of the increase in immunofluorescent intensity is that the density of HCN1 in the plasma membrane of CA1 pyramidal cells dendrites increases as a function of distance from the soma. However, the contribution of a higher relative plasma membrane fraction of the tissue in the stratum lacunosum-moleculare cannot be excluded based on light microscopic data. To determine whether the increased immunostaining of distal dendritic regions is indeed the consequence of a higher immunoreactive HCN1 density in distal dendrites, we applied EM immunogold localizations of HCN1 in these brain regions.

Figure 6. 2. **Light microscopic demonstration of HCN1 immunoreactivity in rat neocortex with HCN1-R (a-c) and HCN1-Gp (d-f) antibodies. (a, d)** Low magnification images of the neocortex and hippocampus. Immunoreactivity is very similar with the two antibodies. Immunoreactive processes are seen in neocortical superficial layers. (**b, e**) Strongly HCN1 immunoreactive apical dendrites of layer V pyramidal cells appear in layer III (e.g. crossed arrows). The strength of reactivity increases toward the apical tufts. Neuropil labelling is stronger with the HCN1-Gp antibody. Note the immunonegativity of the cell bodies. (**c, f**) Higher magnification of the apical dendrites of layer V pyramidal cells revealed that the immunoreactivity is associated with the dendritic plasma membrane (e.g. arrows). Dendritic spines (e.g. arrowheads) are also labelled (see also inset). DG: dentate gyrus; Scale bars: **a, d:** 200 µm; **b, e**: 50 µm; **c, f**: 10 µm.

Fig 6. 2

Subcellular distribution of HCN1 in pyramidal cells

First, we investigated the subcellular distribution of HCN1 in the neocortex (somatosensory) using EM immunoperoxidase and immunogold methods with both of our anti-HCN1 antibodies. Strongly immunopositive apical dendrites and dendritic spines of pyramidal cells dominated the pictures in upper cortical layers. Peroxidase reaction end-product covered the cytoplasm of apical dendrites and spines. No detectable staining was observed in glial processes, in glutamatergic axon terminals and in the cell bodies of nerve cells located in the upper layers. Electron microscopic immunogold analysis demonstrated that the majority of immunoparticles for HCN1 are attached to plasma membranes of apical dendrites and dendritic tufts in upper layers (**Fig. 6. 4a** and **b**). Gold particles were found at the intracellular face of the membranes, in agreement with the intracellular location of the epitopes recognized by our antibodies. The density of HCN1 on the somata and proximal apical dendrites of layer V pyramidal cells was below the detectability of our method. In neocortical pyramidal cells as well as in all other studied cells (CA1 and subicular pyramidal cells), gold particles were not concentrated around asymmetrical synapses on dendritic spines, but were randomly distributed on the extrasynaptic membrane. Similarly, the vicinity of GABAergic synapses on dendritic shafts did not contain an elevated level of gold particles. Both glutamatergic and GABAergic synaptic junctions were always immunonegative with the pre-embedding immunogold method, however this method does not allow us to conclude that the lack of labelling is indeed due to the lack of protein in synaptic junctions (see ref. (Baude et al., 1995; Nusser et al., 1995). Despite our repeated efforts to localize HCN1 with a postembedding immunogold method, no specific labelling could be obtained with our current technique and antibodies. Thus, it remains to be seen whether HCN1 is

Fig. 6. 3. **Double-immunofluorescence labelling of HCN1 with the rabbit (a, c) and guinea pig (b, d) antibodies in hippocampus (a-b) and somatosensory cortex (c-d).**

Identical HCN1 labelling patterns are revealed by the two different antibodies. (**a-b**) The strongest immunolabelling is detected in the subiculum (Sub), followed by the CA1, CA3 areas, and the dentate gyrus (DG). In the CA1 area, the intensity of immunolabelling increases from stratum pyramidale (sp) to stratum lacunosum-moleculare (slm). No detectable immunollabeling is seen in stratum lucidum (sl) of the CA3 area and in the granule cell layer of the dentate gyrus. Weak immunofluorescent signal is found in stratum pyramidale of the CA1 and CA3 regions. (**c-d**) High magnification images of layer II/III of the somatosensory cortex. HCN1 immunolabelling outlines the distal apical dendrites (arrows) and spines (arrowheads) of layer V pyramidal cells, indicating that the majority of immunoreactive HCN1 is present in the plasma membrane. sr: stratum radiatum; so: stratum oriens; Scale bars: **a-b**: 400 μm; **c-d**: 10 μm.

Fig. 6. 3

indeed located exclusively outside the synaptic junctions.

We observed a very similar pattern of labelling in the CA1 area to that of the neocortex. The plasma membranes of distal dendrites of pyramidal cells were strongly outlined by immunoparticles. In the stratum lacunosum-moleculare, dendritic spines also contained detectable levels of HCN1 immunoreactivity, but at a lower density than in shafts (**Fig. 6. 4c** and **d**). However, the somata and the proximal dendrites of CA1 pyramidal cells were mainly immunonegative with the immunogold method similarly to layer V cells. To reveal all subcellular compartments with significant amounts of HCN1 requires the achievement of the highest possible labelling efficiency and finding the cells, which express the highest density of HCN1. As the strongest immunolabelling was observed in the subiculum at the LM level, we turned to this region to investigate the subcellular distribution of HCN1. Indeed, a much higher gold particle density was found in the apical dendrites of subicular pyramidal cells in stratum moleculare compared to the apical tufts of CA1 and layer V pyramidal cells (c.f. **Fig. 6. 4** to **5a, b, e**). In the subiculum, the somatic and proximal dendritic membranes also contained a few gold particles (**Fig. 6. 5c, d, f** and **g**), the density of which seemed to be above of that expected from a random, nonspecific labelling. As in the CA1 area and the neocortex, it was immediately apparent that the density of gold particles was much higher at distal dendrites and spines than on the somata and proximal dendritic shafts and spines. To determine which subcellular compartments contain significant amounts of immunoreactive HCN1 and to estimate the difference in the density of HCN1 in distal and proximal plasma membranes, we quantitatively evaluated the immunogold reactions in the subiculum (see Methods).

Fig. 6. 4. **Electron microscopic immunogold demonstration of the distribution of HCN1 immunoreactivity in the neocortex (a-b) and the hippocampal CA1 area (c-d) with the HCN1-R (a, c) and HCN1-Gp (b, d) antibodies.** (**a-b**) Most gold particles labelling HCN1 are found along dendritic (d) plasma membranes (e.g. arrowheads), presumably originating from layer V pyramidal cells. Gold particles (double arrowheads) are also attached to the plasma membrane of dendritic spines (s). Some particles are present in the cytoplasm of dendrites and spines (e.g. small arrows). No gold particle is associated with an asymmetric synapse (open arrow) and is seen over mitochondria. (**c-d**) A similar pattern of gold particle distribution was found in the stratum lacunosum-moleculare of the hippocampal CA1 area. The plasma membranes of pyramidal cell apical dendrites (d) are strongly labeled (e.g. arrowheads). Much fewer particles are associated with spine membranes (e.g. double arrowheads). The density of immunoparticles was similar in the apical dendrites of layer V and CA1 pyramidal cells, but was lower than that in subicular pyramidal cells. Note that immunoparticles are mainly present on the cytoplasmic side of the dendritic plasma membrane (e.g. arrowheads). Scale bars: **a-b**: 0.4 μm; **c-d**: 0.2 μm.

Fig. 6.4

Quantitative analysis of HCN1 immunogold labelling in subicular pyramidal cells

First, we calculated the nonspecific labelling density in every reaction over the nuclei of pyramidal cells, a subcellular compartment, which should not contain any HCN1. The immunoparticle densities over the nuclei were 0.44±0.26 particles/μm^2 (585±121 μm^2 measured in each animal, n=5 rats) and 0.01±0.01 particles/μm^2 (490±160 μm^2 measured, n=3 rats) for the reactions obtained with the HCN1-R and HCN1-Gp antibodies, respectively. Then we asked which proximal and distal subcellular compartments of pyramidal cells contain significantly higher HCN1 immunoparticle density than the background, nonspecific density. Nine out of the 10 studied subcellular compartments had HCN1 density above background, only the gold particle density of proximal spine cytoplasm did not differ significantly from that obtained over the nuclei (**Fig. 6b** and **c** and **Table 6. 1**). Immunoparticles in the cytoplasm may represent channels being transported to or from the plasma membranes. We often detected gold particles associated with somatic endoplasmic reticulum (**Fig. 6. 5d** and **g**) and Golgi apparatus, rendering the somatic cytoplasmic compartment also a significant pool. The somatic cytoplasm is much larger than the effective somatic plasma membrane, therefore even at a much lower cytoplasmic HCN1 gold density (HCN1-R: 0.23 gold/μm^2 vs. 0.38 gold/μm^2; HCN1-Gp: 0.13 gold/μm^2 vs. 0.47 gold/μm^2 following nonspecific labelling subtraction), the total gold particles could be significantly larger in the cytoplasm. Indeed, we calculated the mean proportion of the gold particles in the somatic cytoplasm to be 91.3±4.8% of the total somatic gold particles. The cytoplasmic pool at distal dendritic and spine compartments (29.1±5.1% and 29.0±12.0%, respectively) was much smaller than at the somatic level, but was still remarkable.

To determine the density differences between distinct proximal and distal plasma membrane compartments of pyramidal cells, we compared immunoparticle densities in those

Fig. 6. 5. **Electron micrographs showing the subcellular distribution of HCN1 immunoreactivity with HCN1-R (a-d) and HCN1-Gp (e-g) antibodies in the subiculum.** (**a**,**b** and **e**) In stratum moleculare, very strong labelling (e.g. arrowheads) is found in the dendritic (d) plasma membranes and a lower particle density is observed in spine (s) membranes (double arrowheads). Some particles are also seen in the cytoplasm (e.g. small arrows). No immunoparticle is associated with asymmetrical synapses (open arrows; perforated synapses: curved arrows). (**c**, **f**) Proximal dendritic shafts (arrowheads) and spine (double arrowheads) have a much lower density of plasma membrane labelling than those located in the stratum moleculare. (**d**, **g**) Gold particle density is similarly low in the somatic plasma membrane (arrows). Few immunoparticles are detected in the somatic cytoplasm, some of which are clearly associated with the membrane of the endoplasmic reticulum (crossed arrows). The nucleus (nuc) contains very few particles. Scale bars: 0.4 μm.

Fig 6.5

	HCN1-R (n=5 rats)				HCN1-Gp (n=3 rats)				HCN1-R (n=5 rats)				HCN1-Gp (n=3 rats)			
	Density (gold/μm^2)		Measured Area (μm^2)		Density (gold/μm^2)		Measured Area (μm^2)		Density (gold/μm)		Measured Length (μm)		Density (gold/μm)		Measured Length (μm)	
	Mean	SD	Mean	SD	Mean	SD	Mean	SD	Mean	SD	Mean	SD	Mean	SD	Mean	SD
Dist DeMe	***26.66***	4.89	10.2	2.1	***23.46***	3.70	8.7	0.5	1.206	0.225	222.4	45.7	1.079	0.170	190.0	10.2
Dist DeCy	***2.32***	0.58	55.6	13.3	**1.64**	0.54	58.7	7.9								
Dist SpMe	***8.24***	2.32	4.1	0.3	**6.12**	3.04	3.7	0.7	0.359	0.107	89.3	6.3	0.281	0.140	80.8	15.8
Dist SpCy	***1.67***	0.50	11.2	1.7	**0.84**	0.31	9.7	2.8								
Prox DeMe	***2.42***	1.05	7.5	1.4	**1.03**	0.49	7.7	0.9	0.091	0.048	162.9	31.3	0.047	0.022	166.5	19.0
Prox DeCy	**0.76**	0.16	37.9	11.3	**0.27**	0.09	47.1	4.9								
Prox SpMe	**1.38**	0.80	4.7	1.3	**0.58**	0.32	3.5	0.2	0.043	0.027	95.6	14.6	0.026	0.015	75.8	4.9
Prox SpCy	0.80	0.56	10.2	1.5	0.14	0.13	6.9	1.0								
SoMe	***0.82***	0.21	21.7	2.1	**0.48**	0.27	15.5	4.0	0.017	0.010	472.8	45.9	0.022	0.012	336.2	86.7
SoCy	**0.67**	0.34	637.1	114.8	**0.14**	0.06	592.3	300.3								
Nucleus	0.44	0.26	584.9	121.3	0.01	0.01	490.4	160.1								

Table 6. 1. **Immunoparticle densities for HCN1 in distinct subcellular compartments of subicular pyramidal cells.**

Bold and italics numbers indicate significance at $p<0.01$, bold numbers at $p<0.05$ using the paired t-test. Abbreviations: DeMe: dendritic plasma membrane, DeCy: dendritic cytoplasm, SpMe: spine plasma membrane, SpCy: spine cytoplasm, SoMe: somatic plasma membrane, SoCy: somatic cytoplasm

plasma membrane compartments, which had significant amounts of HCN1 labeling (Fig. 6. 6b-c insets and Table 6. 1). The density of immunoreactive HCN1 was ~70- and 55-times higher ($p<0.01$ ANOVA; $p<0.05$ paired t-test with Holm correction) in distal dendritic plasma membranes than in somatic membranes for the HCN1-R and HCN1-Gp antibodies, respectively. The 13- and 25-times difference between proximal and distal dendrites for the HCN1-R and HCN1-Gp antibodies, respectively was not the consequence of differences in the diameter of the dendrites, as we have selected small diameter proximal dendrites and found their density very similar to the large diameter proximal apical dendrites. These results demonstrate a distance-dependent increase in the surface density of HCN1 on the somato-dendritic domains of subicular pyramidal cells. However, when the density of immunoreactive HCN1 was compared in the stratum moleculare, we found a 3.3- and 4.3-times higher ($p<0.05$ paired t-test with Holm correction) values in distal dendritic shafts than in spines for the HCN1-R and HCN1-Gp antibodies, respectively. This later finding establishes that not only the distance from the soma, but the actual subcellular domain also plays an important role in determining the surface density of HCN1.

DISCUSSION

Our findings using high-resolution immunolocalization of HCN1 in neocortical, hippocampal, and subicular pyramidal cells demonstrate the uneven axo-somato-dendritic distribution of a

voltage-gated ion-channel. Pyramidal cell axon initial segments, small diameter axons, and axon terminals have an undetectable level of HCN1, whereas somata, proximal and distal dendrites express significant amounts of HCN1 (domain-dependence). Distal dendritic shafts and spines have significantly higher density of HCN1 than proximal shafts and spines of similar diameters, demonstrating that the density of HCN1 increases as a function of distance from the soma (distance-dependence). Furthermore, both proximal and distal dendritic shafts have significantly higher density of HCN1 labeling than spines at the same average distance from the soma, revealing the subcellular compartment-specific regulation of HCN1 surface density (subcellular compartment-dependence). These results establish some new rules in the subcellular distribution of ligand-gated ion-channels on the surface of nerve cells and demonstrate that the cell surface distribution of voltage-gated ion-channels is just as complex and highly regulated as that of ligand-gated channels.

It is important to note that HCN1 is not the only HCN subunit in the CNS. Four subunits (HCN1-4) have been identified so far (Santoro et al., 1997; Gauss et al., 1998; Ludwig et al., 1998; Monteggia et al., 2000) with distinct distribution and functional properties. The homo- or heteromeric assemblies of these subunits are mainly responsible for the functional diversities of I_h (Seifert et al., 1999; Chen et al., 2001). The HCN3 and 4 has an undetectably low level of expression in the hippocampus and the neocortex, but HCN2 is strongly expressed in hippocampal and neocortical pyramidal cells (Moosmang et al., 1999; Bender et al., 2001). The

Fig. 6. 6. **(a) Histogram showing the radial distribution of gold particles around dendritic plasma membranes.** Values along x-axis represent the distance from the center of the gold particle to the center of the plasma membrane (positive sign indicate cytoplasmic side, negative sign extracellular side of the membrane). Bin width: 6 nm. The best Gaussian fit to the data had a peak position at 24 nm in the cytoplasmic side of the membrane and a SD of 11.5 nm.

(**b, c**) Quantitative comparison of immunoreactive HCN1 densities obtained with HCN1-R (**b**) and HCN1-Gp (**c**) antibodies in different subcellular compartments of subicular pyramidal cells. Immunoparticle densities (in 'particle per area', see Methods) are compared in different proximal and distal subcellular compartments (DeMe: dendritic plasma membrane, DeCy: dendritic cytoplasm, SpMe: spine plasma membrane, SpCy: spine cytoplasm, SoMe: somatic plasma membrane, SoCy: somatic cytoplasm) to the non-specific labeling density determined over nuclei (nucl). A significant (black bars: $p<0.01$, gray bars: $p<0.05$; paired t-test) pool of immunoreactive HCN1 was found in all but one (proximal spine cytoplasm) subcellular compartments. Insets illustrate the immunoparticle density (in 'particle per cut membrane length') in plasma membrane compartments that had significant amount of HCN1 labeling. Significant differences are indicated ($p<0.0001$ ANOVA, ** $p<0.01$, * $p<0.05$ paired t-test with Holm correction). Data are given in mean±SD.

fig 6. 6

subcellular distribution of HCN2 in pyramidal cells is similar to that of HCN1 as observed at the light microscopic level (A. Lorincz, T. Notomi, R. Shigemoto, Z. Nusser, unpublished observation), indicating that the organizational principles of the cell surface distribution of HCN1 described in this study are likely to be the same for I_h.

It is well known that the surface of cortical and hippocampal pyramidal cells is subdivided by incoming excitatory and inhibitory inputs (Freund and Buzsaki, 1996; Somogyi et al., 1998a). For example, in the CA1 area, entorhinal inputs terminate in the stratum lacunosum-moleculare and innervate the distal apical tufts of pyramidal cells. Schaffer collaterals innervate the strata oriens and radiatum, and the local axon collaterals of CA1 pyramidal cells mainly form synapses in the stratum oriens. Similarly to the excitatory inputs, the local circuit inhibitory interneurons also provide spatially segregated GABAergic inputs to subicular, hippocampal and neocortical pyramidal cells. Thus, one possibility for the observed gradient in HCN1 density is that presynaptic excitatory and/or inhibitory synaptic inputs influence the density of HCN1 in the postsynaptic plasma membrane. Another possibility may be that the postsynaptic cell provides the clues for the uneven HCN1 densities in a distance- and subcellular compartment-dependent manner. The finding that there is a clear increase in the HCN1 density within stratum radiatum in the hippocampal CA1 area as a function of distance from the stratum pyramidale indicates that the first possibility may not be the case. However, to unequivocally distinguish between the above two possibilities, the location of the presynaptic inputs should be systematically altered (e.g. using genetic approaches) and its effect on the HCN1 densities should be analyzed.

Irrespective of whether the presynaptic inputs are the primary determinants of the uneven HCN1 densities or not, distal synaptic inputs will locally interact with a higher density of I_h than their proximally terminating counterparts. Recent studies elegantly demonstrated the uneven distribution of I_h in pyramidal cell somato-dendritic surface with patch-clamp and imaging techniques (Schwindt and Crill, 1997; Stuart and Spruston, 1998; Tsubokawa et al., 1999; Berger et al., 2001). Our results are in line with those of the above-mentioned functional studies. Here we provide evidence that the augmented I_h is indeed the consequence of an increased HCN1 channel density. Furthermore, by using a high-resolution EM technique, we were able to examine the HCN1 densities in compartments (small caliber secondary and tertiary dendrites and spines), that are inaccessible to patch-clamp methods. By comparing the HCN1 labelling densities in small caliber distal dendrites and in somata, we found a 60-times difference. This is

much larger than the 7-fold difference found by Magee (Magee, 1998) on CA1 pyramidal cells with patch-clamp recordings. This may be due to the fact that, although Magee recorded up to 350 μm away from the soma, the recordings were mainly obtained from relatively large diameter apical dendrites. Although we were unable to quantitatively determine how the HCN1 density increases as a function of distance on the apical dendrites of pyramidal cells, we had the impression that the distance-dependent increase in HCN1 density is not linear.

The uneven HCN1 densities on pyramidal cell dendrites may have several functional consequences (Schwindt and Crill, 1997; Stuart and Spruston, 1998; Magee, 1999a; Williams and Stuart, 2000; Berger et al., 2001). It has been suggested that the increased I_h could contribute to the distance-independent temporal summation of excitatory postsynaptic potentials (EPSPs) (Magee, 1999a; Berger et al., 2001). Similarly, it has been reported that the somatic EPSP time course is independent of the site of generation of the synaptic potential in layer V cortical pyramidal cells, and this is I_h dependent (Williams and Stuart, 2000). Uneven I_h could also determine the extent to which regenerative events are generated in dendrites and how sub- and suprathreshold events propagate to the soma (Schwindt and Crill, 1997; Stuart and Spruston, 1998; Berger et al., 2001). It will be interesting to see how the uneven somato-dendritic I_h influences the time course and temporal summation of hyperpolarizing inhibitory postsynaptic potentials originating from different types of interneurons innervating distinct compartments of the postsynaptic pyramidal cell.

Another novel observation of our study is the significant difference in the HCN1 density between the plasma membrane of dendritic shafts and spines (subcellular compartment-dependence). The lower spine HCN1 density may indicate that the activation/inactivation of I_h may not be synapse specific, but several presynaptic cells converging onto the same dendritic segment will jointly utilize the high I_h density in the small diameter dendrites. The relatively slow time course of I_h kinetics suggests that coincident activation of distal synapses may not be required for their activation; and I_h activated by preceding synaptic activity could selectively alter the efficacy and summation properties of neighboring, distal synapses. Moreover, synapses targeting the spines would be less influenced by local I_h activation than inputs located on dendiritc shafts. Since most GABAergic synapses target dendritic shafts and glutamatergic synapses terminate on the spines this scenario suggests a preferential activation of I_h by GABAergic inputs. Another possibility is that the difference between the HCN1 density in

dendritic shafts and spines may reflect an adaptation to an uneven distribution of some regulatory processes, which requires the close spatial colocalization of the regulatory proteins (e.g. some G protein coupled receptors) and the effector HCN channels. Future studies may test these predictions experimentally.

7. General summary

Central neurons integrate synaptic inputs generated at sites widely distributed across their dendritic tree. The integrative operations of neurons with large dendritic arbors are complex because the impact of distal dendritic inputs on neuronal excitability and axonal AP generation is modified by the passive properties of dendrites, complexity of dendritic morphology together with the distribution of active conductances on the dendritic tree. Despite the thorough investigation of excitatory synaptic integration (reviewed by Williams and Stuart, 2003a), very little is known about that of inhibitory synapses, although they constitute every fifth synapse in the cortex. GABAergic inhibitory cells target specific subcellular compartments of postsynaptic cells. The role of interneurons specifically targeting dendrites is still poorly understood.

This thesis reveals that slow IPSPs in cortical networks arrive from unitary sources, identified as neurogliaform cells, which consistently recruit postsynaptic $GABA_B$ receptors in addition to $GABA_A$ channels. Slow IPSPs generated mainly in dendritic spines increase the inhibitory efficacy of neurogliaform cells in controling excitability of pyramidal cells. It's also shown that electrical, GABAergic, or combined GABAergic and gap junctional signals evoked at dendritic locations are capable of timing somatic action potentials in the network of RSNPCs at behaviorally relevant frequencies. Furthermore the uneven axo-somato-dendritic distribution of a voltage-gated ion channel, HCN1 has been shown. The highest density of HCN1 was found on distal dendritic shafts with decreasing density towars the somata. Since most GABAergic synapses target dendritic shafts and glutamatergic synapses terminate on the spines it suggests a preferential activation of I_h by distal GABAergic inputs.

Identification dendrite targeting interneurons

Combination of biocytin filling during whole-cell patch-clamp recordings of cell pairs with their anatomical analysis following the visualization of biocytin provided a useful tool for investigating the synaptic location dependent effects of identified GABAergic interneurons. We identified two GABAergic interneurons terminating on dendrites, namely regular spiking nonpyramidal (RSNP) cells and late spiking (LS) cells. These cells had distinct firing and anatomical properties. Axonal and dendritic trees of RSNP cells spanned several cortical layers, and showed great morphological heterogeneity. LS cells turned out to form a more homogeneous population based on their anatomical properties. Their dense, subtle and highly ramifying axonal

trees and short, rarely branching dendritic arbours were rather confined to the layers containing parent somata and LS cells were identified as neurogliaform cells. Both cells innervated preferably dendritic spines and shafts. Furthermore, in their identified connections RSNP and neurogliaform cells placed their synapses on dendrites at similar distances from postsynaptic somata.

Functional impact of neurogliaform and RSNP cells

Since being strongly attenuated during their propagation to the cell body, distal inhibitory synaptic inputs have been considered to have no effect on the generation of the axonal action potentials. Excitatory synapses innervate dendritic spines, therefore RSNPs and neurogliaform cells can inhibit EPSPs, thus effectively control dendritic excitability. This influence of neurogliaform cells is further enhanced by their ability to place their synapses on the origin of spine neck, where a more powerful control of EPSPs has been proposed (Qian and Sejnowski, 1990). In addition, neurogliaform cells evoked combined postsynaptic $GABA_A$ and $GABA_B$ receptor-mediated resposnes resulting in slow IPSPs that could further increase their inhibitory efficacy. Slow IPSPs can provide a wide temporal window for summation of coincident inhibitory inputs, thus increasing the impact of distal inhibitory inputs on neuronal output.

Recent studies have revealed that perisomatic inhibitory inputs could modify neuronal output by timing the axonal action potentials (Tamas et al., 2000) and it's dependent on the type of connection (Tamas et al., 2000). Dendritic networks of RSNP cells revealed here could effectively time axonal spikes and it was also connection specific. Similarly to basket cells (Tamas et al., 2000), chemical synapses alone were not effective in timing the firing of postsynaptic cells. Electrical connections were only efficient, when mediated by many gap junctions and precise timing was achieved when cells were interconnected with combined GABAergic and electrical synapses. In conjunction with the subcellular position of the synapses, other factors like the composition of the postsynaptic GABA receptors and the type of connection construct the efficacy of dendritic inhibitory inputs.

The position specific effect of inhibitory synapses can also depend on the distribution of voltage-gated ion channels they interact with. Hyperpolarization of postsynaptic membrane potential caused by IPSPs can activate HCN channels. Subcellular distribution of HCN1, a subunit of HCN was investigated in cortical pyramidal cells. Applying a quantitative immunogold method, we have revealed some basic rules governing the cell surface distribution

of HCN1. Pyramidal cell axons have an undetectable level of HCN1, whereas somata and dendrites express significant amounts of HCN1 (domain-dependence). Distal dendrites have significantly higher density of HCN1 than somata and proximal dendrites, demonstrating that the density of HCN1 increases as a function of distance from the soma (distance-dependence). Furthermore, dendritic shafts have significantly higher density of HCN1 labeling than spines at the same average distance from the soma, revealing the subcellular compartment-specific regulation of HCN1 surface density (subcellular compartment-dependence). Since GABAergic interneurons target specific domains and subcellular regions, they can interact with different amount of I_h.

Future implications

Synapses of neurogliaform cells were only effective in releasing GABA when presynaptic cells fired at very low rate, suggesting a physiological role tuned for sparse temporal operation and for metabotropic receptors activating an array of biochemical pathways. Ongoing network activity can provide a dynamic pattern of excitatory and inhibitory inputs on a neurogliaform cell that can switch on and off neurogliaform synapses by altering its firing rate. It's also possible that certain neuromodulators are needed to strengthen neurogliaform synapses.

Ongoing activity refines electrical compartmentalization of dendrites. Regarding that the opening probability of gap junctions is voltage-dependent; it's possible that actual network activity can recruit different numbers of gap junctions in the network of RSNP cells, therefore controling the impact of RSNP cells on the neuronal output. Future studies will investigate these possibilities under various behavioral conditions.

There can be differences in the inhibitory efficacy of dendritic GABAergic synapses depending on the type of the postsynaptic cell as well. It can be due to the differential expression and cell surface distribution of voltage-gated ion channels in distinct cell classes. It would be interesting to investigate the HCN1 distribution on aspiny interneurons, where in contrast to pyramidal cells, excitatory and inhibitory inputs share the same subcellular compartment (dendritic shaft).

Revealing the axo-somato-dendritic distribution of other voltage-gated ion channels essentials in signal propagation, like Na^+-, K^+-, and Ca^{2+}-channels would further increase our knowledge on their effect on the integrative functions of dendrites. Different subcellular location of distinct isoforms may contribute to different functions. For example, certain isoforms of

voltage-gated Na^+-channels ($Na_v1.1$-$Na_v1.9$) might be specific for axon initial segments and nodes of Ranvier and support the formation and propagation of action potentials, whereas other isoforms specific for dendrites can support backpropagating action potentials.

Future experiments will better define distribution of voltage-gated ion channels and their relation to the synaptic properties.

8. Összefoglalás

Az agykérget felépítő idegsejtek összetett dendritfával rendelkeznek, melyek serkentő és gátló szinapszisok ezreit fogadják. A központi idegrendszeri neuronok egyik alapvető funkciója a szinaptikus integráció. Ennek során a dendritfa több ezer szinapszisból származó információt dolgoz fel és továbbít a sejttest felé, melynek eredményeképp a sejtek kimenetét meghatározó akciós potenciál keletkezik. A dendritfa különböző területeire érkező szinapszisoknak a sejtek serkenthetőségére és az axonális akciós potenciálokra tett hatását számos körülmény határozza meg. A dendritfa elektrotónusos tulajdonságai, összetett morfológiája és az aktív konduktanciák változatos sejtfelszíni eloszlása befolyásolja a szinaptikus információ feldolgozását. A dendritekre érkező serkentő bemeneteket részletesen tanulmányozták az elmúlt évtizedben (Williams and Stuart, 2003a), kevés adat áll azonban rendelkezésre a GABA-erg, gátló bemenetek hatásáról, bár ezek alkotják az agykérgi szinapszisok mintegy 20 %-át. A GABA-erg interneuronok a posztszinaptikus sejtek eltérő sejtrégióit innerválják kizárólag dendriteket innerváló GABA-erg interneuronok szerepe még nem tisztázott.

A disszertációban leírt kísérletek bizonyítják, hogy az agykérgi hálózatokban megjelenő lassú IPSP-k lehetnek egysejt eredetűek, mivel a vizsgált neurogliaform sejtek egyöntetűen kombinált $GABA_A$ és $GABA_B$ receptorok által közvetített válaszokat váltottak ki a posztszinaptikus piramissejteken. A főként dendrittüskéken létrehozott lassú IPSP-k kiváltásával a neurogliaform sejtek helyben képesek befolyásolni a piramissejtekre szintén a dendrittüskékre érkező serkentő bemenetek hatékonyságát. Kísérleteink azt is kimutatják, hogy a dendritiken lévő elektromos, GABA-erg, vagy kombinált GABA-erg és elektromos szinapszisok képesek a szomatikus akciós potenciálok időzítésére szabályosan tüzelő nem piramissejtek (RSNP sejtek) hálózataiban. Sikerült kvantitatív különbségeket feltárni egy hiperpolarizáció-aktivált feszültségfüggő ioncsatorna, a HCN1 sejtfelszíni eloszlásában piramissejteken, amely legnagyobb sűrűségben disztális dendrittörzseken mértünk. Minthogy a GABA-erg szinapszisok főként dendrittörzsön, a glutamáterg szinapszisok pedig dendrittüskén helyezkednek el el, ez arra utal, hogy a csatornát preferenciálisan aktiválhatják disztális GABA-erg bemenetek.

A dendriteket innerváló interneuronok azonosítása

A sejtpárokból történő whole-cell patch-clamp elvezetések kombinálása a sejtpárok ezt követő vizualizálásával és anatómiai analízisével hasznos eszköznek bizonyult a GABA-erg szinapszisok pozíció-függő hatásának vizsgálatához. Sikerült azonosítani két GABA-erg sejttípust, az RSNP

sejteket és a későn tüzelő (LS) sejteket, amelyek dendriteket innerváltak. Ezek a sejtek meghatározott fiziológiai és anatómiai jellegzetességekkel bírtak. Az RSNP sejtek axonfelhői és dendritfái számos rétegbe átterjedtek és nagy morfológiai heterogenitást mutattak. Az LS sejtek anatómiai tulajdonságaik alapján homogén populációt képeztek. Sűrű, szövevényes axonfelhőjük és alig elágazó, rövid dendritjeik alapján, melyek kiterjedése főként a sejttestet tartalmazó rétegre korlátozódott, neurogliaform sejtekként voltak azonosíthatók. Mindkét sejttípus elsősorban dendrittüskéket és dendrittörzseket innervált. Azonosított kapcsolataikban az RSNP és neurogliaform sejtek a posztszinaptikus sejttestől hasonló távolságra létesítettek kapcsolatokat a posztszinaptikus dendritfán.

A neurogliaform sejtek és RSNP sejtek funkcionális jelentősége

A disztálisan érekző, gátló szinaptikus bemenetekről az a nézet alakult ki, hogy nincs hatásuk az axonális akciós potenciál képzésre, mert a sejttest felé történő terjedésük során erősen csökken az amplitúdójuk és lassul a kinetikájuk. A serkentő bemenetek főként dendrittüskékre érkeznek, így az RSNP és neurogliaform sejtek képesek az EPSP-k helyi gátlására hatékony ellenőrzés alatt tartva a dendritek serkenthetőségét. A neurogliaform sejtek hatását tovább fokozhatja, hogy szinapszisaik egy része a tüskenyak eredésére érkezik, ahol az EPSP-k hatékonyabban konrollálhatók (Qian and Sejnowski, 1990). A neurogliaform sejtek ezen felül kombinált $GABA_A$ és $GABA_B$ receptor közvetített válszokat váltottak ki, ezzel tovább erősítve a tüskékre érkező gátlás hatékonyságát (Qian and Sejnowski, 1990). A lassú IPSP-k széles időablakot kínálnak a gátló bemenetek összeadódásához, így növelhetik a disztális dendriteken lévő gátló szinapszisok hatását a szomatikus és axonális akciós potenciálok keletkezésére.

A periszomatikus gátló szinapszisok képesek az akciós potenciálok időzítésére (Tamas et al., 2000) és ez függ a szinaptikus kapcsolat típusától (Tamas et al., 2000). Kimutattuk, hogy a dendriteken elhelyezkedő szinapszisok is képesek a szomatikus-axonális akciós potenciálok időzítésére. Az RSNP sejtek itt feltárt dendritikusan kapcsolódó hálózataiban a kosársejtekhez hasonlóan (Tamas et al., 2000), a kémiai szinapszisok egyedül nem voltak képesek a posztszinapstikus sejt tüzelését időzíteni. Az elektromos szinapszisok csak nagyszámú gap junction esetén (n=8) voltak hatékonyak, és csak az elekromos és kémiai szinapszisok kombinációjával volt elérhető a posztszinaptikus tüzelés precíz időzítése. A szinapszisok

szubcelluláris elhelyezkedése mellett tehát a szinaptikus kapcsolat típusa is hozzájárul a dendritikus gátló bemenetek hatékonyságához.

A gátló szinapszisok pozíciófüggő hatását a feszültségfüggő ioncsatornák szubcelluláris elhelyezkedése is befolyásolja. Az IPSP-k okozta hiperpolarizáció aktiválja az erre érzékeny, ún. hiperpolarizáció aktivált és ciklikus nukleotid-függő kation csatornákat (HCN). A HCN egyik alegységének, a HCN1-nek szubcelluláris eloszlását piramissejteken vizsgáltuk. Egy kvantitatív immunoarany módszer alkalmazásával sikerült néhány, a HCN1 sejtfelszíni eloszlását leíró szabályszerűséget feltárni. A HCN1 sejtrégió specifikusan helyezkedett el piramissejteken, mivel axonjaikkal ellentétben a piramissejtek sejttestje és dendritfája szignifikáns mennyiségben tartalmaztott HCN1-et. A disztális dendritekben szignifikánsan nagyobb HCN1 sűrűséget mértünk, mint a sejttesteken és a proximális dendriteken. A HCN1 szubcelluláris eloszlásában tehát a sejttesttől való távolság is meghatározó fontosságú. A sejttesttől ugyanazon távolságra elhelyezkedő dendrittörzsek és dendrittüskék HCN1 tartalmában megfigyelt különbség pedig a HCN1 eloszlás szubcelluláris kompartment függését mutatja. Mivel a GABA-erg sejtek a piramissejtek specifikus sejtrégióit innerválják, ennek megfelelően különböző mennyiségű HCN csatornát aktiválhatnak.

Előretekintés

A neurogliaform szinapszisok csak alacsony frekvenciákú aktivitás mellett szabadítottak fel hatákonyan GABA-t, ami arra utal, hogy a neurogliaform szinapszisok működésfüggő plaszticitása a metabotróp posztszinaptikus folymatokra hangolt. A hálózati háttéraktivitás a neurogliaform sejtekre érkező serkentő és gátló bementek dinamikus mintázatát biztosítja, amely a hálózat állapotának megfelelően a neurogliaform sejtek tüzelési frekvenciájának módosításán keresztül ki- és bekapcsolhatja ezek szinapszisait. Az is lehetséges, hogy bizonyos neuromodulátorok szükségesek a neurogliaform szinapszisok megbízhatóságának növeléséhez. Az állandó szinaptikus háttéraktivitás tovább finomíthatja a dendritek elektromos kompartmentalizációját. Tekintve, hogy a gap junction-ok nyitási valószínűsége feszülségfüggő, elképzelhető, hogy az éppen aktuális hálózati háttéraktivitás eltérő számú gap junction-t nyit ki az RSNP sejtek kapcsolataiban, ezáltal szabályozva az RSNP sejtek posztszinaptikus sejtaktivitásra tett hatását. Ezen lehetőségek vizsgálata jövőbeli kísérletekben lehetséges.

A dendritikus GABA-erg szinapszisok gátlási hatékonyságában eltérések lehetnek a posztszinaptikus sejt típusától függően is. Ez többek között annak köszönhető, hogy egyes feszültségfüggő ioncsatornák expressziója és sejtfelszíni eloszlása sejttípustól függően is eltérő lehet. Érdekes lenne például megvizsgáni a HCN1 sejtfelszíni eloszlását különböző interneuronokon, melyekről ismert, hogy nincs vagy csak nagyon kevés dendrittüskéjük van, ezáltal a piramissejtekkel ellentétben, az interneuronokra érkező serkentő és gátló bemenetek hasonló szubcelluláris kompartmenteken osztoznak. További jelterjedésben fontos feszülségfüggő ioncsatornák, mint a feszültségfüggő Na^+-, K^+-, és Ca^{2+}- csatornák és izoformáik axo-szomato-dendritikus eloszlásának vizsgálata nagyban segítené a dendritek integratív funkcióinak megismerését. Bizonyos feszültségfüggő Na^+-csatorna ($Na_v1.1$-$Na_v1.9$) izoformák például specifikusan az axon iniciális szegmentumon és a Ranvier-féle nóduszon elhelyezkedve az akciós potenciálok keletkezését és terjedédét támogathatják, míg más specifikusan dendriteken lévő izoformák az akciós potenciálok dendritekbe történő visszaterjedédét segíthetik.

9. References

Alonso G, Widmer H (1997) Clustering of KV4.2 potassium channels in postsynaptic membrane of rat supraoptic neurons: an ultrastructural study. Neuroscience 77:617-621.

Andersen P, Dingledine R, Gjerstad L, Langmoen IA, Laursen AM (1980) Two different responses of hippocampal pyramidal cells to application of gamma-amino butyric acid. J Physiol 305:279-296.

Andrasfalvy BK, Magee JC (2001) Distance-dependent increase in AMPA receptor number in the dendrites of adult hippocampal CA1 pyramidal neurons. J Neurosci 21:9151-9159.

Banks MI, Li TB, Pearce RA (1998) The synaptic basis of GABAA,slow. J Neurosci 18:1305-1317.

Barnard EA, Skolnick P, Olsen RW, Mohler H, Sieghart W, Biggio G, Braestrup C, Bateson AN, Langer SZ (1998) International Union of Pharmacology. XV. Subtypes of gamma-aminobutyric acidA receptors: classification on the basis of subunit structure and receptor function. Pharmacol Rev 50:291-313.

Baude A, Nusser Z, Molnar E, McIlhinney RA, Somogyi P (1995) High-resolution immunogold localization of AMPA type glutamate receptor subunits at synaptic and non-synaptic sites in rat hippocampus. Neuroscience 69:1031-1055.

Benardo LS (1994) Separate activation of fast and slow inhibitory postsynaptic potentials in rat neocortex in vitro. J Physiol (Lond) 476:203-215.

Bender RA, Brewster A, Santoro B, Ludwig A, Hofmann F, Biel M, Baram TZ (2001) Differential and age-dependent expression of hyperpolarization-activated, cyclic nucleotide-gated cation channel isoforms 1-4 suggests evolving roles in the developing rat hippocampus. Neuroscience 106:689-698.

Berger T, Larkum ME, Luscher HR (2001) High I(h) channel density in the distal apical dendrite of layer V pyramidal cells increases bidirectional attenuation of EPSPs. J Neurophysiol 85:855-868.

Bernander O, Douglas RJ, Martin KA, Koch C (1991) Synaptic background activity influences spatiotemporal integration in single pyramidal cells. Proc Natl Acad Sci U S A 88:11569-11573.

Bischofberger J, Schild D (1995) Different spatial patterns of [Ca2+] increase caused by N- and L-type Ca2+ channel activation in frog olfactory bulb neurones. J Physiol 487 (Pt 2):305-317.

Bischofberger J, Jonas P (1997) Action potential propagation into the presynaptic dendrites of rat mitral cells. J Physiol 504 (Pt 2):359-365.

Bowery NG, Bettler B, Froestl W, Gallagher JP, Marshall F, Raiteri M, Bonner TI, Enna SJ (2002) International Union of Pharmacology. XXXIII. Mammalian gamma- aminobutyric acid(B) receptors: structure and function. Pharmacol Rev 54:247-264.

Buhl EH, Halasy K, Somogyi P (1994) Diverse sources of hippocampal unitary inhibitory postsynaptic potentials and the number of synaptic release sites. Nature 368:823-828.

Buzsaki G (1996) The hippocampo-neocortical dialogue. Cerebral Cortex 6:81-92.

Buzsaki G, Chrobak JJ (1995) Temporal structure in spatially organized neuronal ensembles: a role for interneuronal networks. Curr Opin Neurobiol 5:504-510.

Buzsaki G, Leung L-W, Vanderwolf CH (1983) Cellular bases of hippocampal EEG in the behaving rat. Brain Res Rev 6:139-171.

Cajal SRy (1894) Les nouvelles idee`s sur la srtucture du systeme` nerveux chez l`homme et chez les verte`bre`s (New Ideas on the Structure of the Nervous System of Man and the Vertebrates. Cambridge: MIT Press.

Cajal SRy (1904) Textura del systema nervioso del hombre y los vertebrados. Madrid: Moya, N.

Cauli B, Porter JT, Tsuzuki K, Lambolez B, Rossier J, Quenet B, Audinat E (2000) Classification of fusiform neocortical interneurons based on unsupervised clustering. Proc Natl Acad Sci U S A 97:6144-6149.

Cauli B, Audinat E, Lambolez B, Angulo MC, Ropert N, Tsuzuki K, Hestrin S, Rossier J (1997) Molecular and physiological diversity of cortical nonpyramidal cells. J Neurosci 17:3894-3906.

Chen S, Wang J, Siegelbaum SA (2001) Properties of hyperpolarization-activated pacemaker current defined by coassembly of HCN1 and HCN2 subunits and basal modulation by cyclic nucleotide. J Gen Physiol 117:491-504.

Christie BR, Eliot LS, Ito K, Miyakawa H, Johnston D (1995) Different Ca2+ channels in soma and dendrites of hippocampal pyramidal neurons mediate spike-induced Ca2+ influx. J Neurophysiol 73:2553-2557.

Christie MJ, Williams JT, North RA (1989) Electrical coupling synchronizes subthreshold activity in locus coeruleus neurons in vitro from neonatal rats. J Neurosci 9:3584-3589.

Cobb SR, Buhl EH, Halasy K, Paulsen O, Somogyi P (1995) Synchronization of neuronal activity in hippocampus by individual GABAergic interneurons. Nature 378:75-78.

Cohen I, Navarro V, Clemenceau S, Baulac M, Miles R (2002) On the origin of interictal activity in human temporal lobe epilepsy in vitro. Science 298:1418-1421.

Colbert CM, Johnston D (1996) Axonal action-potential initiation and Na+ channel densities in the soma and axon initial segment of subicular pyramidal neurons. J Neurosci 16:6676-6686.

Colbert CM, Johnston D (1998) Protein kinase C activation decreases activity-dependent attenuation of dendritic Na+ current in hippocampal CA1 pyramidal neurons. J Neurophysiol 79:491-495.

Condorelli DF, Belluardo N, Trovato-Salinaro A, Mudo G (2000) Expression of Cx36 in mammalian neurons. Brain Res Brain Res Rev 32:72-85.

Connors BW, Benardo LS, Prince DA (1983) Coupling between neurons of the developing rat neocortex. J Neurosci 3:773-782.

Conti F, Weinberg RJ (1999) Shaping excitation at glutamatergic synapses. Trends Neurosci 22:451-458.

Cossart R, Dinocourt C, Hirsch JC, Merchan-Perez A, De Felipe J, Esclapez M, Bernard C, Ben-Ari Y (2001) Dendritic but not somatic GABAergic inhibition is decreased in experimental epilepsy. Nat Neurosci 4:52-62.

Craig AM, Boudin H (2001) Molecular heterogeneity of central synapses: afferent and target regulation. Nat Neurosci 4:569-578.

Cutting GR, Lu L, O'Hara BF, Kasch LM, Montrose-Rafizadeh C, Donovan DM, Shimada S, Antonarakis SE, Guggino WB, Uhl GR, et al. (1991) Cloning of the gamma-aminobutyric acid (GABA) rho 1 cDNA: a GABA receptor subunit highly expressed in the retina. Proc Natl Acad Sci U S A 88:2673-2677.

De Schutter E (1992) A consumer guide to neuronal modeling software. Trends Neurosci 15:462-464.

Deiters O (1865) Untersuchungen u¨ ber Gehirn und Ru¨ckenmark des Menschen und der Sa¨ ugethiere. Braunschweig.
Destexhe A, Sejnowski TJ (1995) G protein activation kinetics and spillover of gamma-aminobutyric acid may account for differences between inhibitory responses in the hippocampus and thalamus. Proc Natl Acad Sci U S A 92:9515-9519.
Draguhn A, Traub RD, Schmitz D, Jefferys JG (1998) Electrical coupling underlies high-frequency oscillations in the hippocampus in vitro. Nature 394:189-192.
Dutar P, Nicoll RA (1988) A physiological role for GABAB receptors in the central nervous system. Nature 332:156-158.
Eccles JC, Libet B, Young RR (1958) The behavior of chromatolysed motoneurons studied by intracellular recording. J Physiol (Lond) 143:11-41.
Fisahn A, Pike FG, Buhl EH, Paulsen O (1998) Cholinergic induction of network oscillations at 40 Hz in the hippocampus in vitro. Nature 394:186-189.
Freund TF, Buzsaki G (1996) Interneurons of the hippocampus. Hippocampus 6:347-470.
Fricker D, Miles R (2000) EPSP amplification and the precision of spike timing in hippocampal neurons. Neuron 28:559-569.
Fritschy JM, Weinmann O, Wenzel A, Benke D (1998) Synapse-specific localization of NMDA and GABA(A) receptor subunits revealed by antigen-retrieval immunohistochemistry. J Comp Neurol 390:194-210.
Fritschy JM, Meskenaite V, Weinmann O, Honer M, Benke D, Mohler H (1999) GABAB-receptor splice variants GB1a and GB1b in rat brain: developmental regulation, cellular distribution and extrasynaptic localization. Eur J Neurosci 11:761-768.
Fukuda T, Kosaka T (2000) Gap junctions linking the dendritic network of GABAergic interneurons in the hippocampus. J Neurosci 20:1519-1528.
Fukuda T, Kosaka T (2003) Ultrastructural study of gap junctions between dendrites of parvalbumin-containing GABAergic neurons in various neocortical areas of the adult rat. Neuroscience 120:5-20.
Galarreta M, Hestrin S (1999) A network of fast-spiking cells in the neocortex connected by electrical synapses. Nature 402:72-75.
Gauss R, Seifert R, Kaupp UB (1998) Molecular identification of a hyperpolarization-activated channel in sea urchin sperm. Nature 393:583-587.
Gibson JF, Beierlein M, Connors BW (1999) Two networks of electrically coupled inhibitory neurons in neocortex. Nature 402:75-79.
Golgi C (1886) Sulla Fina Anatomica degli Organti Centrali del Sistema Nervoso. Milan: Hoepli.
Gulledge AT, Stuart GJ (2003) Excitatory actions of GABA in the cortex. Neuron 37:299-309.
Gulyas AI, Hajos N, Freund TF (1996) Interneurons containing calretinin are specialized to control other interneurons in the rat hippocampus. J Neurosci 16:3397-3411.
Gulyas AI, Megias M, Emri Z, Freund TF (1999) Total number and ratio of excitatory and inhibitory synapses converging onto single interneurons of different types in the CA1 area of the rat hippocampus. J Neurosci 19:10082-10097.
Gupta A, Wang Y, Markram H (2000) Organizing principles for a diversity of GABAergic interneurons and synapses in the neocortex [see comments]. Science 287:273-278.
Harris KM (1999) Structure, development, and plasticity of dendritic spines. Curr Opin Neurobiol 9:343-348.
Hausser M, Mel B (2003) Dendrites: bug or feature? Curr Opin Neurobiol 13:372-383.

Hausser M, Spruston N, Stuart GJ (2000) Diversity and dynamics of dendritic signaling. Science 290:739-744.

Hestrin S, Armstrong WE (1996) Morphology and physiology of cortical neurons in layer I. J Neurosci 16:5290-5300.

Hille B (2001) Ionic channels of excitable membranes. Sunderland: Sinauer Associates Inc.

Hoffman DA, Johnston D (1998) Downregulation of transient K+ channels in dendrites of hippocampal CA1 pyramidal neurons by activation of PKA and PKC. J Neurosci 18:3521-3528.

Hoffman DA, Magee JC, Colbert CM, Johnston D (1997) K+ channel regulation of signal propagation in dendrites of hippocampal pyramidal neurons. Nature 387:869-875.

Hu H, Shao LR, Chavoshy S, Gu N, Trieb M, Behrens R, Laake P, Pongs O, Knaus HG, Ottersen OP, Storm JF (2001) Presynaptic Ca2+-activated K+ channels in glutamatergic hippocampal terminals and their role in spike repolarization and regulation of transmitter release. J Neurosci 21:9585-9597.

Isaacson JS, Solis JM, Nicoll RA (1993) Local and diffuse synaptic actions of GABA in the hippocampus. Neuron 10:165-175.

Jefferys JGR, Traub RD, Whittington MA (1996) Neuronal networks for induced '40 Hz' rhythms. Trends Neurosci 19:202-208.

Johnston D, Hoffman DA, Magee JC, Poolos NP, Watanabe S, Colbert CM, Migliore M (2000) Dendritic potassium channels in hippocampal pyramidal neurons. J Physiol 525 Pt 1:75-81.

Jones EG (1975) Varieties and distribution of non-pyramidal cells in the somatic sensory cortex of the squirrel monkey. J Comp Neurol 160:205-268.

Kawaguchi Y, Kubota Y (1996) Physiological and morphological identification of somatostatin- or vasoactive intestinal polypeptide-containing cells among GABAergic cell subtypes in rat frontal cortex. J Neurosci 16:2701-2715.

Kawaguchi Y, Kubota Y (1997) GABAergic cell subtypes and their synaptic connections in rat frontal cortex. Cereb Cortex 7:476-486.

Klausberger T, Roberts JD, Somogyi P (2002) Cell type- and input-specific differences in the number and subtypes of synaptic GABA(A) receptors in the hippocampus. J Neurosci 22:2513-2521.

Koch C, Segev I (2000) The role of single neurons in information processing. Nat Neurosci 3 Suppl:1171-1177.

Koos T, Tepper JM (1999) Inhibitory control of neostriatal projection neurons by GABAergic interneurons. Nat Neurosci 2:467-472.

Krnjevic K, Schwartz S (1967) The action of gamma-aminobutyric acid on cortical neurones. Exp Brain Res 3:320-336.

Kulik A, Nakadate K, Nyiri G, Notomi T, Malitschek B, Bettler B, Shigemoto R (2002) Distinct localization of GABA(B) receptors relative to synaptic sites in the rat cerebellum and ventrobasal thalamus. Eur J Neurosci 15:291-307.

Lacaille J-C, Schwartzkroin PA (1988) Stratum lacunosum-moleculare interneurons of hippocampal CA1 region. II. Intrasomatic and intradendritic recordings of local circuit synaptic interactions. J Neurosci 8:1411-1424.

Larkum ME, Zhu JJ, Sakmann B (1999) A new cellular mechanism for coupling inputs arriving at different cortical layers. Nature 398:338-341.

Larkum ME, Zhu JJ, Sakmann B (2001) Dendritic mechanisms underlying the coupling of the dendritic with the axonal action potential initiation zone of adult rat layer 5 pyramidal neurons. J Physiol 533:447-466.

Lisman JE, Idiart MAP (1995) Storage of 7±2 short-term memories in oscillatory subcycles. Science 267:1512-1515.

Llinás R, Nicholson C (1971) Electroresponsive properties of dendrites and somata in alligator Purkinje cells. J Neurophysiol 34:32-551.

Llinás R, Sugimori M (1980) Electrophysiological properties of in vitro Purkinje cell dendrites in mammalian cerebellar slices. J Physiol (Lond) 305:197-213.

Llinás R, Nicholson C, Freeman JA, Hillman DE (1968) Dendritic spikes and their inhibition in alligator Purkinje cells. Science 160:1132-1135.

Lopez-Bendito G, Shigemoto R, Kulik A, Paulsen O, Fairen A, Lujan R (2002) Expression and distribution of metabotropic GABA receptor subtypes GABABR1 and GABABR2 during rat neocortical development. Eur J Neurosci 15:1766-1778.

Lorente de Nó R, Coundouris GA (1959) Decremental conduction in peripheral nerve integration of stimuli in the neuron. Proc Natl Acad Sci 45:592-617.

Ludwig A, Zong X, Jeglitsch M, Hofmann F, Biel M (1998) A family of hyperpolarization-activated mammalian cation channels. Nature 393:587-591.

Lytton WW, Sejnowski TJ (1991) Simulations of cortical pyramidal neurons synchronized by inhibitory interneurons. J Neurophysiol 66:1059-1079.

Maccaferri G, McBain CJ (1996) The hyperpolarization-activated current (Ih) and its contribution to pacemaker activity in rat CA1 hippocampal stratum oriens-alveus interneurones. J Physiol 497:119-130.

Magee J, Hoffman D, Colbert C, Johnston D (1998) Electrical and calcium signaling in dendrites of hippocampal pyramidal neurons. Annu Rev Physiol 60:327-346.

Magee JC (1998) Dendritic hyperpolarization-activated currents modify the integrative properties of hippocampal CA1 pyramidal neurons. J Neurosci 18:7613-7624.

Magee JC (1999a) Dendritic lh normalizes temporal summation in hippocampal CA1 neurons. Nat Neurosci 2:508-514.

Magee JC (1999b) Distribution of voltage-gated ion channels. In: Dendrites (G. Stuart NS, M., Ha¨usser, eds), p 139–160. Oxford: Oxford Univ. Press.

Magee JC, Johnston D (1995) Characterization of single voltage-gated Na+ and Ca2+ channels in apical dendrites of rat CA1 pyramidal neurons. J Physiol 487 (Pt 1):67-90.

Magee JC, Cook EP (2000) Somatic EPSP amplitude is independent of synapse location in hippocampal pyramidal neurons. Nat Neurosci 3:895-903.

Mainen ZF, Sejnowski TJ (1995) Reliability of spike timing in neocortical neurons. Science 268:1503-1506.

Mann-Metzer P, Yarom Y (1999) Electrotonic coupling interacts with intrinsic properties to generate synchronized activity in cerebellar networks of inhibitory interneurons. J Neurosci 19:3298-3306.

McCullogh WS, Pitts WH (1943) A logical calculus of the ideas immanent in nervous activity. BullMathByophys 5.

McNamara NM, Muniz ZM, Wilkin GP, Dolly JO (1993) Prominent location of a K+ channel containing the alpha subunit Kv 1.2 in the basket cell nerve terminals of rat cerebellum. Neuroscience 57:1039-1045.

Meskenaite V (1997) Calretinin-immunorective local circuit neurons in area 17 of the cynomolgus monkey, Macaca fascicularis. J Comp Neurol 379:113-132.
Migliore M, Shepherd GM (2002) Emerging rules for the distributions of active dendritic conductances. Nat Rev Neurosci 3:362-370.
Miles R, Toth K, Gulyas AI, Hajos N, Freund TF (1996) Differences between somatic and dendritic inhibition in the hippocampus. Neuron 16:816-823.
Misgeld U, Bijak M, Jarolimek W (1995) A physiological role for GABAB receptors and the effects of baclofen in the mammalian central nervous system. Prog Neurobiol 46:423-462.
Mody I, De Koninck Y, Otis TS, Soltesz I (1994) Bridging the cleft at GABA synapses in the brain. Trends Neurosci 17:517-525.
Monteggia LM, Eisch AJ, Tang MD, Kaczmarek LK, Nestler EJ (2000) Cloning and localization of the hyperpolarization-activated cyclic nucleotide-gated channel family in rat brain. Brain Res Mol Brain Res 81:129-139.
Moosmang S, Biel M, Hofmann F, Ludwig A (1999) Differential distribution of four hyperpolarization-activated cation channels in mouse brain. Biol Chem 380:975-980.
Niedermeyer E, Lopes da Silva F (1993) Electroencephalography: Basic Principles, Clinical Applications and Related Fields. Baltimore: Williams and Wilkins.
Nusser Z (1999) In: Dendrites (Stuart G, Spruston N, Ha¨usser M, eds), p 85–113. Oxford: Oxford Univ. Press.
Nusser Z, Cull-Candy S, Farrant M (1997) Differences in synaptic GABA(A) receptor number underlie variation in GABA mini amplitude. Neuron 19:697-709.
Nusser Z, Sieghart W, Somogyi P (1998a) Segregation of different GABAA receptors to synaptic and extrasynaptic membranes of cerebellar granule cells. J Neurosci 18:1693-1703.
Nusser Z, Hajos N, Somogyi P, Mody I (1998b) Increased number of synaptic GABA(A) receptors underlies potentiation at hippocampal inhibitory synapses. Nature 395:172-177.
Nusser Z, Sieghart W, Benke D, Fritschy JM, Somogyi P (1996) Differential synaptic localization of two major gamma-aminobutyric acid type A receptor alpha subunits on hippocampal pyramidal cells. Proc Natl Acad Sci U S A 93:11939-11944.
Nusser Z, Roberts JD, Baude A, Richards JG, Sieghart W, Somogyi P (1995) Immunocytochemical localization of the alpha 1 and beta 2/3 subunits of the GABAA receptor in relation to specific GABAergic synapses in the dentate gyrus. Eur J Neurosci 7:630-646.
Nusser Z, Lujan R, Laube G, Roberts JD, Molnar E, Somogyi P (1998c) Cell type and pathway dependence of synaptic AMPA receptor number and variability in the hippocampus. Neuron 21:545-559.
Nyiri G, Freund TF, Somogyi P (2001) Input-dependent synaptic targeting of alpha(2)-subunit-containing GABA(A) receptors in synapses of hippocampal pyramidal cells of the rat. Eur J Neurosci 13:428-442.
Oakley JC, Schwindt PC, Crill WE (2001) Dendritic calcium spikes in layer 5 pyramidal neurons amplify and limit transmission of ligand-gated dendritic current to soma. J Neurophysiol 86:514-527.
Obata K, Oide M, Tanaka H (1978) Excitatory and inhibitory actions of GABA and glycine on embryonic chick spinal neurons in culture. Brain Res 144:179-184.
Ottersen OP, Landsend AS (1997) Organization of glutamate receptors at the synapse. Eur J Neurosci 9:2219-2224.

Overstreet LS, Jones MV, Westbrook GL (2000) Slow desensitization regulates the availability of synaptic GABA(A) receptors. J Neurosci 20:7914-7921.

Oviedo H, Reyes AD (2002) Boosting of neuronal firing evoked with asynchronous and synchronous inputs to the dendrite. Nat Neurosci 5:261-266.

Pare D, Shink E, Gaudreau H, Destexhe A, Lang EJ (1998) Impact of spontaneous synaptic activity on the resting properties of cat neocortical pyramidal neurons In vivo. J Neurophysiol 79:1450-1460.

Pearce RA (1993) Physiological evidence for two distinct GABAA responses in rat hippocampus. Neuron 10:189-200.

Peters A, Sethares C (1997) The organization of double bouquet cells in monkey striate cortex. J Neurocytol 26:779-797.

Peters A, Palay SF, Webster HDF (1991) The Fine Structure of the Nervous System. New York: Oxford Univ. Press.

Petralia RS, Rubio ME, Wenthold RJ (1998) Selectivity in the distribution of glutamate receptors in neurons. Cell Biol Int 22:603-608.

Qian N, Sejnowski TJ (1990) When is an inhibitory synapse effective? Proc Natl Acad Sci USA 87:8145-8149.

Rall W (1958) Dendritic current distribution and whole neuron properties. NaMedResInstResRep NM0105.01.02:479-525.

Rall W (1977) Cellular Biology of Neurons, Section1. In: Handbook of Physiology.The Nervous system., pp 39-79: American Physiological Society.

Reyes A, Lujan R, Rozov A, Burnashev N, Somogyi P, Sakmann B (1998) Target-cell-specific facilitation and depression in neocortical circuits. Nat Neurosci 1:279-285.

Rhodes KJ, Monaghan MM, Barrezueta NX, Nawoschik S, Bekele-Arcuri Z, Matos MF, Nakahira K, Schechter LE, Trimmer JS (1996) Voltage-gated K+ channel beta subunits: expression and distribution of Kv beta 1 and Kv beta 2 in adult rat brain. J Neurosci 16:4846-4860.

Rouach N, Avignone E, Meme W, Koulakoff A, Venance L, Blomstrand F, Giaume C (2002) Gap junctions and connexin expression in the normal and pathological central nervous system. Biol Cell 94:457-475.

Rozental R, Giaume C, Spray DC (2000) Gap junctions in the nervous system. Brain Res Brain Res Rev 32:11-15.

Rubio ME, Wenthold RJ (1997) Glutamate receptors are selectively targeted to postsynaptic sites in neurons. Neuron 18:939-950.

Salmelin R, Hamalainen M, Kajola M, Hari R (1995) Functional segregation of movement-related rhythmic activity in the human brain. Neuroimage 2:237-243.

Santoro B, Grant SG, Bartsch D, Kandel ER (1997) Interactive cloning with the SH3 domain of N-src identifies a new brain specific ion channel protein, with homology to eag and cyclic nucleotide-gated channels. Proc Natl Acad Sci U S A 94:14815-14820.

Santoro B, Liu DT, Yao H, Bartsch D, Kandel ER, Siegelbaum SA, Tibbs GR (1998) Identification of a gene encoding a hyperpolarization-activated pacemaker channel of brain. Cell 93:717-729.

Schaefer AT, Larkum ME, Sakmann B, Roth A (2003) Coincidence detection in pyramidal neurons is tuned by their dendritic branching pattern. J Neurophysiol 89:3143-3154.

Schwindt PC, Crill WE (1997) Modification of current transmitted from apical dendrite to soma by blockade of voltage- and Ca2+-dependent conductances in rat neocortical pyramidal neurons. J Neurophysiol 78:187-198.

Seifert R, Scholten A, Gauss R, Mincheva A, Lichter P, Kaupp UB (1999) Molecular characterization of a slowly gating human hyperpolarization- activated channel predominantly expressed in thalamus, heart, and testis. Proc Natl Acad Sci U S A 96:9391-9396.

Sekirnjak C, Martone ME, Weiser M, Deerinck T, Bueno E, Rudy B, Ellisman M (1997) Subcellular localization of the K+ channel subunit Kv3.1b in selected rat CNS neurons. Brain Res 766:173-187.

Shepherd GM (1990) The Synaptic Organization of the Brain. New York: Oxford Univ. Press.

Shepherd GM (1996) The dendritic spine: a multifunctional integrative unit. J Neurophysiol 75:2197-2210.

Shigemoto R, Kinoshita A, Wada E, Nomura S, Ohishi H, Takada M, Flor PJ, Neki A, Abe T, Nakanishi S, Mizuno N (1997) Differential presynaptic localization of metabotropic glutamate receptor subtypes in the rat hippocampus. J Neurosci 17:7503-7522.

Singer W (1993) Synchronization of cortical activity and its putative role in information processing and learning. Ann Rev Physiol 55:349-374.

Singer W, Gray CM (1995) Visual feature integration and the temporal correlation hypothesis. Annu Rev Neurosci 18:555-586.

Sloper JJ, Powell TPS (1978) Dendro-dendritic and reciprocal synapses in the primate motor cortex. Proc R Soc Lond B 203:23-38.

Somogyi P (1977) A specific 'axo-axonal' interneuron in the visual cortex of the rat. Brain Res 136:345-350.

Somogyi P, Cowey A (1981) Combined Golgi and electron microscopic study on the synapses formed by double bouquet cells in the visual cortex of the cat and monkey. J Comp Neurol 195:547-566.

Somogyi P, Hodgson AJ (1985) Antisera to gamma-aminobutyric acid. III. Demonstration of GABA in Golgi-impregnated neurons and in conventional electron microscopic sections of cat striate cortex. J Histochem Cytochem 33:249-257.

Somogyi P, Freund TF, Cowey A (1982) The axo-axonic interneuron in the cerebral cortex of the rat, cat and monkey. Neuroscience 7:2577-2607.

Somogyi P, Nunzi MG, Gorio A, Smith AD (1983) A new type of specific interneuron in the monkey hippocampus forming synapses exclusively with the axon initial segments of pyramidal cells. Brain Res 259:137-142.

Somogyi P, Tamas G, Lujan R, Buhl EH (1998a) Salient features of synaptic organisation in the cerebral cortex. Brain Res Rev 26:113-135.

Somogyi P, Nusser Z, Roberts JDB, Lujan R (1998b) Precision and variability in the placement of pre- and postsynaptic receptors in relation to neurotransmitter release sites. In: HFSP, pp 82-93. Strasbourg.

Spencer WA, Kandel ER (1961) Electrohysiology of hippocampal neurons: IV. Fast prepotentials. J Neurophysiol 24:272-285.

Spruston N, Jaffe DB, Johnston D (1994) Dendritic attenuation of synaptic potentials and currents: the role of passive membrane properties. Trends Neurosci 17:161-166.

Spruston N, Schiller Y, Stuart G, Sakmann B (1995) Activity-dependent action potential invasion and calcium influx into hippocampal CA1 dendrites. Science 268:297-300.

Steriade M, McCormick DA, Sejnowski TJ (1993) Thalamocortical oscillations in the sleeping and aroused brain. Science 262:679-685.
Steriade M, Amzica F, Contreras D (1996) Synchronization of fast (30-40 Hz) spontaneous cortical rhythms during brain activation. J Neurosci 16:392-417.
Steward O, Falk PM, Torre ER (1996) Ultrastructural basis for gene expression at the synapse: synapse-associated polyribosome complexes. J Neurocytol 25:717-734.
Stuart G, Hausser M (1994) Initiation and spread of sodium action potentials in cerebellar Purkinje cells. Neuron 13:703-712.
Stuart G, Spruston N (1998) Determinants of voltage attenuation in neocortical pyramidal neuron dendrites. J Neurosci 18:3501-3510.
Stuart G, Spruston N, Sakmann B, Hausser M (1997) Action potential initiation and backpropagation in neurons of the mammalian CNS. Trends Neurosci 20:125-131.
Stuart GJ, Sakmann B (1994) Active propagation of somatic action potentials into neocortical pyramidal cell dendrites. Nature 367:69-72.
Takumi Y, Ramirez-Leon V, Laake P, Rinvik E, Ottersen OP (1999) Different modes of expression of AMPA and NMDA receptors in hippocampal synapses. Nat Neurosci 2:618-624.
Tamas G, Buhl EH, Somogyi P (1997) Fast IPSPs elicited via multiple synaptic release sites by distinct types of GABAergic neuron in the cat visual cortex. J Physiol (Lond) 500:715-738.
Tamas G, Somogyi P, Buhl EH (1998) Differentially interconnected networks of GABAergic interneurons in the visual cortex of the cat. J Neurosci 18:4255-4270.
Tamas G, Buhl EH, Lorincz A, Somogyi P (2000) Proximally targeted GABAergic synapses and gap junctions synchronize cortical interneurons. Nat Neurosci 3:366-371.
Thomson AM, Destexhe A (1999) Dual intracellular recordings and computational models of slow inhibitory postsynaptic potentials in rat neocortical and hippocampal slices. Neuroscience 92:1193-1215.
Thomson AM, West DC, Hahn J, Deuchars J (1996) Single axon IPSPs elicited in pyramidal cells by three classes of interneurones in slices of rat neocortex. J Physiol 496:81-102.
Traub RD, Whittington MA, Stanford IM, Jefferys JGR (1996) A mechanism for generation of long-range synchronous fast oscillations in the cortex. Nature 383:621-624.
Traub RD, Kopell N, Bibbig A, Buhl EH, LeBeau FE, Whittington MA (2001) Gap junctions between interneuron dendrites can enhance synchrony of gamma oscillations in distributed networks. J Neurosci 21:9478-9486.
Tsubokawa H (2000) Control of Na+ spike backpropagation by intracellular signaling in the pyramidal neuron dendrites. Mol Neurobiol 22:129-141.
Tsubokawa H, Miura M, Kano M (1999) Elevation of intracellular Na+ induced by hyperpolarization at the dendrites of pyramidal neurones of mouse hippocampus. J Physiol 517 (Pt 1):135-142.
Turner RW, Meyers DE, Richardson TL, Barker JL (1991) The site for initiation of action potential discharge over the somatodendritic axis of rat hippocampal CA1 pyramidal neurons. J Neurosci 11:2270-2280.
Valverde F (1971) Short axon neuronal subsystems in the visual cortex of the monkey. Int J Neurosci 1:181-197.

Venance L, Rozov A, Blatow M, Burnashev N, Feldmeyer D, Monyer H (2000) Connexin expression in electrically coupled postnatal rat brain neurons. Proc Natl Acad Sci U S A 97:10260-10265.

Vetter P, Roth A, Hausser M (2001) Propagation of action potentials in dendrites depends on dendritic morphology. J Neurophysiol 85:926-937.

Watanabe M, Fukaya M, Sakimura K, Manabe T, Mishina M, Inoue Y (1998) Selective scarcity of NMDA receptor channel subunits in the stratum lucidum (mossy fibre-recipient layer) of the mouse hippocampal CA3 subfield. Eur J Neurosci 10:478-487.

Williams SR, Stuart GJ (2000) Site independence of EPSP time course is mediated by dendritic I(h) in neocortical pyramidal neurons. J Neurophysiol 83:3177-3182.

Williams SR, Stuart GJ (2002) Dependence of EPSP efficacy on synapse location in neocortical pyramidal neurons. Science 295:1907-1910.

Williams SR, Stuart GJ (2003a) Role of dendritic synapse location in the control of action potential output. Trends Neurosci 26:147-154.

Williams SR, Stuart GJ (2003b) Voltage- and site-dependent control of the somatic impact of dendritic IPSPs. J Neurosci 23:7358-7367.

Yamazaki M, Matsuo R, Fukazawa Y, Ozawa F, Inokuchi K (2001) Regulated expression of an actin-associated protein, synaptopodin, during long-term potentiation. J Neurochem 79:192-199.

Yuste R, Denk W (1995) Dendritic spines as basic functional units of neuronal integration. Nature 375:682-684.

Yuste R, Tank DW (1996) Dendritic integration in mammalian neurons, a century after Cajal. Neuron 16:701-716.

Zigmond MJ, Bloom FE, Landis SC, Roberts JL, Squire LR (1999) Fundamental Neuroscience. San Diego: Academic Press.

10. Acknowledgments

First of all, I would like to thank my supervisors, Gábor Tamás and Zoltán Nusser for the sharp criticism and for the support, motivation and enthusiasm they transmitted to me during these years.

Gábor, for showing me how to explore the secrets of cortical interneurons with light- and electronmicroscopy, and for making it possible to take my first steps in the investigation of synaptic neurotransmission in his laboratory in Szeged. The electrohysiological experiments and suggestion of the HCN project that has become an important part of my thesis are also appreciated.

Zoli, for introducing me in pre-, and postembedding immunohystochemistry in his professional way. Thank you for the HCN project, and the interesting brainstorming sessions during coffee breaks in the office, that I believe have broadened my theoretical and practical view.

I'd also like to thank the members of the laboratory in Szeged for the friendly and stimulating enviroment. János Szabadics for the electrophysiological experiments, Éva Tóth for the excellent technical assistance, Anna Simon for her anatomical contribution and Szabolcs Oláh.

Many thanks to the members of the laboratory in Budapest. Attila Losonczy, Noémi B. Holderith, Mihály Köllő and Ágota Bíró for the inspiring enviroment and great conversations. Andrea Zöldi for the excellent technical assistance.

My greatest thanks is reserved for those who helped the most with their support and love, my parents and my brother, Laca. They belief in me has allowed me to achieve my goals and go far beyond my expectations.

Special thanks to Máté, for his continuous support and encouragement. It still amazes me that he decided to share his life with me.

My best friends and *partners in crime*, Bazsi and Nóra for the holidays we spent together. You always cheer me up in hard times.

Last, but not least I'd like to thank all the members and students of the Department of Comparative Physiology in University of Szeged, where I've spent more than 5 years. Especially, Margó Várady, our secretry for her help in administrative issues, Gabriella Mészáros for taking care of animals, and Ferenc Gyulai for his help whenever I encountered technical problems.

11. Publications

Tamás, G., **Lőrincz, A.**, Simon, A and Szabadics, J. (2003) Identified sources and targets of slow inhibition in the neocortex. *Science* 299, 1902-1905

Lőrincz, A., Notomi, T., Tamás, G., Shigemoto,R and Nusser, Z (2002): Polarized and compartment-dependent distribution of HCN1 in pyramidal cell dendrites. *Nature Neuroscience* 5, 1185-1193

Szabadics, J., **Lőrincz, A.**, Tamás, G.(2001): Beta and gamma frequency synchronization by dendritic GABAergic synapses and gap junction in a network of cortical interneurons. *Journal of Neuroscience* 21, 5824-5831

Tamás, G., Buhl, E. H**., Lőrincz, A**. and Somogyi, P. (2000): Proximally targeted GABAergic synapses and gap junctions synchronize cortical interneurons. *Nature Neuroscience* 3, 366-371.

Conference posters:

Lőrincz, A., Szabadics, J Simon, A and Tamás, G. (2003) Identified sources and targets of slow inhibition in the neocortex. *IBRO Congress,* Prague, 2003 July

Lőrincz, A., Tamás, G. and Nusser, Z (2002): Polarized and compartment-dependent distribution of HCN1 in pyramidal cell dendrites. *Society for Neuroscience Annual Meeting*, Orlando, 2002 Nov

Lőrincz, A., Szabadics, J., Tamás, G.(2002): Beta and gamma frequency synchronization by dendritic GABAergic synapses and gap junction in a network of cortical interneurons. Meeting of the *Hungarian Society for Neuroscience,* 2002 Jan

Tamás, G., **Lőrincz, A**., Szabadics, J., Buhl E.H., and Somogyi, P.(2000): Synchronization of cortical interneurons by perisomatic and denritic mechanisms. In *Workshop on Dendrites (New York) pp. 75 Ed.: R. Yuste, S.A. Sigelbaum*

Tamás, G., **Lőrincz, A.,** Szabadics, J., Buhl E.H., Somogyi, P.(2000): Perisomatic and dendritic mechanisms of synchronisation in identified cortical interneuron-interneuron connections. *J Physiol (Lond)* 526P: 18S Meeting of *Hungarian Physiological Society and The Physiological Society,* Budapest, 2000 May

Tamás, G., **Lőrincz, A.,** Szabadics, J., Buhl E.H., and Somogyi, P.(2000): Differential transmission os gamma frequency activity between neocortical interneurons. *GABA 2000 Conference, Cairns pp. 7*